

8. SITE 1147¹

Shipboard Scientific Party²

BACKGROUND AND OBJECTIVES

The objective of Site 1147 was to recover a continuous sequence of the uppermost hemipelagic sediments (75 meters below seafloor [mbsf]) near Site 1148 (SCS-5C), so that the near-surface sediments lost to slumping or channeling at Site 1148 could be recovered.

Site 1147 is located at 18°50.11'N, 116°33.28'E, at shotpoint 1940 on *JOIDES Resolution* seismic Line 5C-2 at a water depth of ~3245 m (Fig. F9, p. 53, in the “Leg 184 Summary” chapter; see also Figs. F5, p. 17, F15, p. 30, F16A, p. 31, F16B, p. 32, and F17B, p. 34, all in the “Seismic Stratigraphy” chapter). The site is ~0.45 nmi upslope from Site 1148 (the revised location of SCS-5C).

The repositioning of Site SCS-5C to shotpoint 1980 on *JOIDES Resolution* seismic Line 5C-2 placed the site location in the scar of a surface slump. Interpretation of the seismic records suggests that from 10 to 20 m of sediment are missing and that the disturbance to the sediment column may extend downward another 20 to 30 m. Site 1147 was proposed to recover the uppermost sediments, which are missing or disturbed at Site 1148. Correlation among multisensor track (MST) and color spectral reflectance (CSR) data at these two sites indicates a maximum of 7 m of missing section at the top of Site 1148 relative to Site 1147. A continuous, distinct, and undisturbed reflector at ~0.08 seconds below seafloor (~60 mbsf) can be easily traced between Sites 1147 and 1148.

¹Examples of how to reference the whole or part of this volume.

²Shipboard Scientific Party addresses.

OPERATIONS

Site 1147 (Proposed Site SCS-5F)

During operations at Site 1146, the vessel received approval for coring Site 1147 (newly proposed site SCS-5F) to a depth of 100 mbsf. This site was less than one mile west of Site 1148 (proposed site SCS-5C). The plan was to piston core three holes to a depth of ~80 mbsf to recover the upper part of the Pleistocene section that, judging from seismic records, appeared to be missing at Site 1148. The 40-nmi transit to Site 1147 took 4 hr at an average speed of 9.5 kt. The beacon was dropped on Global Positioning System coordinates at 1035 hr on 29 March. The corrected precision depth recorder referenced to the dual elevator stool was 3256.4 m.

Hole 1147A

Hole 1147A was spudded with the advanced hydraulic piston corer (APC) at 1815 hr on 29 March. The seafloor depth was inferred at 3257.5 m from the recovery of the first core. Piston coring advanced with nine APC cores to 81.4 mbsf with an average recovery of 100.4% (Tables [T1](#), [T2](#), both also in [ASCII format](#)). Cores were oriented starting with Core 3H.

Hole 1147B

The vessel was moved in dynamic positioning mode 10 m east of Hole 1147A. Hole 1147B was spudded with the APC at 0245 hr on 30 March. The inferred seafloor depth was 3257.0 m. Piston coring advanced with nine APC cores to 85.5 mbsf with an average recovery of 100.0% (Tables [T1](#), [T2](#)). Cores were oriented starting with Core 3H.

Hole 1147C

The ship was moved 10 m east of Hole 1147B. Hole 1147C was spudded with the APC at 1045 hr on 30 March. The inferred seafloor depth was 3256.9 m. Piston coring advanced with nine APC cores to 78.6 mbsf with an average recovery of 97.5% (Tables [T1](#), [T2](#)). Cores were oriented starting with Core 2H.

The total recovery for this site was 243.8 m, or 99.3% of the cored interval of 245.5 m. After the bit was pulled clear of the seafloor at 1820 hr on 30 March, it was raised ~50 m above the seafloor in preparation for the move to Site 1148. After the beacon was released and recovered at 1915 hr, the *JOIDES Resolution* was moved to Site 1148, ~0.5 nmi east of Site 1147, in dynamic positioning mode.

COMPOSITE SECTION

We built a continuous meters composite depth (mcd) scale and a splice (as defined in "[Composite Section](#)," p. 3, in the "Explanatory Notes" chapter) that range from the top of Core 184-1147B-1H to the bottom of Section 184-1147B-9H-6. The splice and the mcd extend from 0 to 90.73 mcd and span the entire cored sequence.

Site 1147 was drilled in order to recover a slumped section missing from Site 1148, as described in "[Background and Objectives](#)," p. 1. A

T1. Site 1147 coring summary, p. 31.

T2. Site 1147 coring summary by section, p. 32.

continuous mcd and splice can be constructed for the local region if data are combined from Site 1147 and nearby Site 1148. The correlation is accomplished by tying Sample 184-1147C-6H-4, 112 cm (49.22 mcd), to Sample 184-1148B-5H-5, 32 cm (46.57 mcd).

The mcd scale and the splice are based on the stratigraphic correlation of whole-core MST and split-core CSR data (lightness, L^*) collected at 4- to 5-cm intervals (see “Physical Properties,” p. 9, for details). From the MST, we used magnetic susceptibility (MS), gamma-ray attenuation (GRA) bulk density, and natural gamma radiation (NGR) data. These data and the splice constructed from them are presented on the mcd scale in Figures F1, F2, F3, and F4 (also as Synergy Software KaleidaGraph plots and Microsoft Excel data files [see the “Supplementary Materials” contents list]; the spliced records are also available in ASCII format). The depth offsets that comprise the mcd scale are given in Table T3 (also in ASCII format). The splice tie points (Table T4, also in ASCII format) should be used as a guide for detailed postcruise sampling.

Magnetic susceptibility data were the most useful stratigraphic tool for correlation at this site. Natural gamma radiation and CSR data were helpful in intervals where structure in the MS profile was ambiguous.

We constructed the mcd scale by assuming that the uppermost sediment (the “mudline”) in Core 184-1147B-1H was the sediment/water interface. This core, the “anchor” in the composite depth scale, has the same depth on both the mbsf and mcd scales. We correlated downhole from this anchor, core by core, until we reached the bottom of Hole 1147B, the deepest penetration at the site.

LITHOSTRATIGRAPHY

Lithologic Units

Unit I (0.0–91.7 mcd)

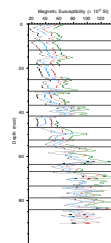
Interval: Cores 184-1147A-1H through 9H; Cores 184-1147B-1H through 9H; Cores 184-1147C-1H through 9H

Depth: 0–81.4 mbsf (Hole 1147A); 0–85.5 mbsf (Hole 1147B); 0–78.6 mbsf (Hole 1147C)

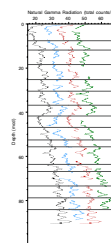
Age: Pleistocene

Only one lithologic unit was identified at Site 1147 (Fig. F5). Unit I is composed of clay with quartz and smaller amounts of nannofossils. A few intervals display a notable increase in lightness, apparent by visual observation and in the lightness L^* index of the spectrophotometric data (Fig. F5). The increases in lightness correspond to increases in nannofossil abundance as observed in smear slides. These lighter intervals are also characterized by an increase in the occurrence of green clay layers, higher foraminifer content, and intense bioturbation. An ~3-cm-thick reddish brown oxidized sediment layer, with a dusky brown manganese precipitation zone at the base, is observed at the top of Cores 184-1147A-1H, 184-1147B-1H, and 184-1147C-1H. This interval probably represents the modern seafloor.

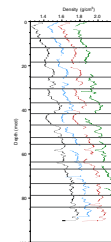
F1. Smoothed/correlated MS data and splice, p. 11.



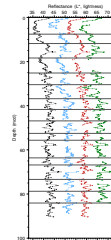
F2. Smoothed/correlated NGR data and splice, p. 12.



F3. Smoothed/correlated GRA data and splice, p. 13.



F4. Smoothed/correlated L^* values from the CSR data and splice, p. 14.



T3. Composite depths, p. 33.

T4. Site 1147 splice tie points, p. 34.

Carbonate-Rich Intervals

Slightly lighter intervals with higher carbonate content are observed, but these are less pronounced than at Site 1146, and many of them are observed only in the spectrophotometric data. Visible light-colored layers are compiled in Table T5. Typical features of the light layers include abundant foraminifers visible on the core surface, common green clay layers (typically 1–3 cm thick), well-defined bioturbation, and slightly yellowish gray patches or mottles, which represent traces of bioturbation. Smear-slide estimates indicate calcareous nannofossil contents of >10%, compared to around 0%–5% in the background clay.

Green Layers and Mottles

Green layers and irregular green mottles occur frequently and are well developed in the upper part of the hole, reaching a maximum frequency above ~40 mcd. From this maximum, the green layers decrease in frequency downhole, being rare at the base of the drilled section (Fig. F5). The layers are characterized by a clay that is stiffer than the dominant clay lithology of the section, and they have a lower water content and higher *P*-wave velocity.

Bioturbation

Bioturbation is intense throughout the cored interval. The sediment is generally completely homogenized, and individual burrows are observed only in exceptional cases. Pyrite-filled burrows are the exception to this pattern. They occur at a frequency of one to two burrows per section in the upper part of the unit and increase in frequency downhole (Fig. F5). Large pyrite-filled burrows reach several centimeters in length and as much as 2 cm in diameter. Pyrite-filled burrows first appear at ~48 mcd, and no “iron sulfides” are found above ~38 mcd. Pyrite-filled burrows are probably formed by the diagenetic replacement of organic matter-rich burrow fills.

Volcaniclastic Layers

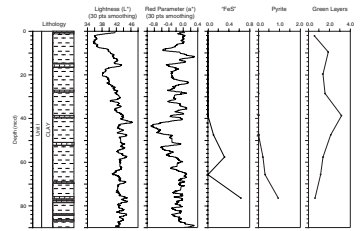
Well-preserved distinct volcanic ash layers are missing at Site 1147. However, we observed occurrences of volcanic ash as burrow fill (finely dispersed within the sediment), as isolated pumice clasts, and as thin layers (Table T6). The maximum ash layer thickness is ~1 cm. The poorly preserved ash layering is probably a result of the intensive bioturbation observed in all three holes at Site 1147.

BIOSTRATIGRAPHY

Calcareous Nannofossils

Pleistocene sediments recovered at Site 1147 yielded common to abundant calcareous nannofossils having poor to good preservation. Variations in nannofossil preservation and abundance at different levels indicate changes in calcite dissolution caused by fluctuations of the lysocline (Fig. F6). Nannofossil biostratigraphy at this site is based on a detailed study of samples taken from core catchers and from within cores of Hole 1147A (Tables T7, T8).

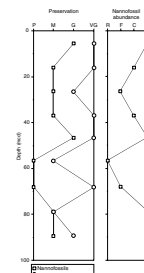
F5. Site 1147 section summary, p. 15.



T5. Light-colored, carbonate-rich layers, p. 35.

T6. Volcanic ash layers, p. 36.

F6. Nannofossil and foraminifer preservation and abundance, p. 16.



T7. Summary of biohorizons, p. 37.

T8. Calcareous nannofossil checklist, p. 38.

Five calcareous nannofossil bioevents were documented in the 89.4-m Pleistocene sediment sequence of Hole 1147A (Tables T7, T8). The oldest bioevent, the first occurrence (FO) of the *Gephyrocapsa* (small) acme interval, was observed at 78.8 mcd. No *Helicosphaera sellii* was found below that level, which suggests that the age at the bottom of Hole 1147A (89.4 mcd, Sample 1147A-9H-CC) is older than 1.22 Ma but younger than 1.47 Ma.

Planktonic Foraminifers

Planktonic foraminifers were examined in all core-catcher samples from Hole 1147A and selected core-catcher samples from Hole 1147B (see Table T9). Site 1147 yields a moderate abundance of planktonic foraminifers although their preservation degrades from very good to moderate downsection, as documented by an increase in planktonic foraminiferal fragments (Fig. F6).

The relatively high sedimentation rates at Site 1147 and the depth of the drilled section limit the number of biohorizons used to date the cores. Because *Globorotalia truncatulinoides* occurs continuously down the full length of this hole, this interval is assigned to biozone N22 (Blow, 1969). The absence of *Globigerinoides fistulosus* constrains the age of the sediments in Hole 1147A to younger than 1.77 Ma. Within Zone N22 we used the last occurrence (LO) (0.12 Ma; Thompson et al., 1979) and FO (0.40 Ma; Li, 1997) of pink *Globigerinoides ruber* as two biostratigraphic control points (Table T7).

Benthic Foraminifers

Site 1147 also yields rare to few deep-sea benthic foraminifers. One benthic foraminiferal datum, the LO of *Stilostomella*, was observed at 68.06 mcd and indicates an age of ~0.75 Ma based on the latitude of this site (Schönfeld, 1996).

Summary

At Site 1147, both planktonic foraminifers and calcareous nannofossils are common to abundant. Foraminiferal preservation degraded from very good to moderate downsection, whereas nannofossils exhibited poor to good preservation. Benthic foraminifers are generally few in number.

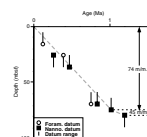
An age-depth plot of the three fossil groups shows that the biohorizons generally agree with each other (Fig. F7). The age of the oldest sediments recovered at Site 1147 is estimated at 1.22–1.47 Ma. The sedimentation rate at Site 1147, calculated based on biostratigraphic data (Table T7; Fig. F7), is 75 m/m.y. after 1 Ma and 23 m/m.y. between 1.01 and 1.22 Ma.

PALEOMAGNETISM

Shipboard paleomagnetic measurements for Holes 1147A, 1147B, and 1147C consisted of long-core measurements of the natural remanent magnetization (NRM) at 8-cm intervals before and after alternating field demagnetization up to 20 mT, which was carried out on the archive halves of all APC cores. In addition, 41 discrete samples were collected from the working halves of Hole 1147A at an average spacing

T9. Planktonic foraminifer check-list, p. 39.

F7. Age-depth plot, p. 17.



of one sample per section (1.5 m). Cores 184-1147A-3H through 9H, 184-1147B-3H through 9H, and 184-1147C-3H through 9H were oriented using the Tensor tool.

Hole 1147A

Long-core measurements of NRM and subsequent demagnetization steps were carried out at 8-cm intervals with two demagnetization steps at 10 and 20 mT.

The direction of the NRM (after demagnetization at 20 mT and correction using the Tensor tool data where available) is shown in Figure F8. Above 59 mcd, declination and inclination generally oscillate around values expected for a geocentered dipole field at this latitude (0° and 38° , respectively), with an amplitude consistent with the secular variation of the geomagnetic field. At 59.3 mcd, the Brunhes/Matuyama boundary is identified by a sudden swing of the declination to 180° and a change in inclination to negative values. The upper Jaramillo transition occurs at 72 mcd; the lower, at 76.1 mcd. A short period of reverse declinations and inclinations follows the lower Jaramillo between 76.1 and 80.7 mcd. Below 79.5 mcd to the bottom of Hole 1147A (88.5 mcd), the data are highly scattered, and no further magnetostratigraphic information could be obtained. Table T10 shows a summary of the magnetostratigraphic information for this site as well as sedimentation rates based on polarity transitions.

Hole 1147B

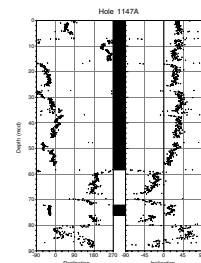
Long-core measurements were made at Hole 1147B at 8-cm intervals, with one demagnetization step of 10 mT for Cores 184-1147B-1H through 4H and two demagnetization steps of 10 and 20 mT for Cores 184-1147B-5H through 9H (Fig. F9). The Brunhes/Matuyama boundary was encountered at a depth of 57.4 mcd. Farther downcore, the upper Jaramillo transition occurred at 70.8 mcd; the lower Jaramillo, at 76.1 mcd. Besides these transitions, a declination change of 90° was noted between 63.4 and 64.9 mcd. This 90° change occurs only in Section 184-1147B-7H-2. The section was inspected, and no evidence was found that it was split 90° off normal.

Hole 1147C

Long-core measurements were made at Hole 1147C at 8-cm intervals, with one demagnetization step of 10 mT for Cores 184-1147C-1H through 5H and two demagnetization steps of 10 and 20 mT for Cores 184-1147C-6H through 9H. The Brunhes/Matuyama boundary was found at a depth of 57 mcd. Farther downcore, the upper Jaramillo transition occurred at 72.3 mcd; the lower, at 76.1 mcd (Fig. F10).

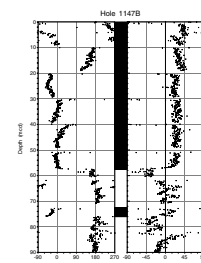
The results from all three holes correlate very well, with the exception of the 90° declination shift that occurs only in Hole 1147B. Because it is found in only one of these holes and is contained in one complete section, we believe this shift is an artifact and should be disregarded.

F8. Declination and inclination for Hole 1147A, 0–88.5 mcd, p. 18.

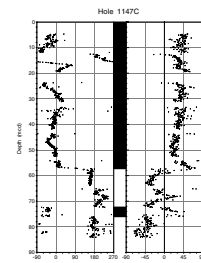


T10. Age-depth relationship from the magnetic polarity time scale, p. 40.

F9. Declination and inclination for Hole 1147B, p. 19.



F10. Declination and inclination for Hole 1147C, p. 20.



SEDIMENTATION AND ACCUMULATION RATES

Site 1147 reached only 1.22–1.47 Ma at the bottom of the drilled holes, and only 11 datum levels were used for its chronostratigraphy: three paleomagnetic (Table T10), five nannofossil, two planktonic, and one benthic foraminiferal (Table T7) events.

Although the age covered is similar to that of Site 1144, the sedimentation rates and, in particular, the accumulation rates of Site 1147 are much less variable (Fig. F11) (also given as Synergy Software KaleidaGraph plots and Microsoft Excel data files [see the “Supplementary Materials” contents list]). The total sedimentation rate is higher in the last 0.26 m.y. (96 m/m.y.), but the carbonate and noncarbonate accumulation rates remain fairly constant throughout the hole and average ~ 0.7 g/cm²/k.y. and 4–5 g/cm²/k.y., respectively (Table T11).

ORGANIC GEOCHEMISTRY

Summary

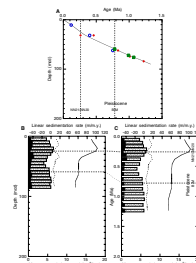
Only trace amounts of methane (<10 ppmv) and no other hydrocarbon gases were detected in sediments at Site 1147. This mirrors low concentrations found in the upper sediments of the other low-productivity sites drilled in the northern South China Sea.

Sampling and analysis for inorganic carbon (IC), total carbon (TC), nitrogen, and sulfur in Hole 1147A were conducted as described in “Organic Geochemistry,” p. 14, in the “Explanatory Notes” chapter. Carbonate varies from 4.4 to 30.5 wt% (average [AV] = 12.8 wt%; standard deviation [SD] = 6.0), with all values <20 wt% with the exception of Sample 184-1147A-4H-6, 107–108 cm. No downhole trend is observed (Table T12; Fig. F12A). Total organic carbon (TOC) concentration by difference (TC – IC) declines markedly from 1.21 wt% at the top of the hole to 0.58 wt% at 12 mcd. A more gradual decline is noted downhole, with values of <0.4 wt% (AV = 0.56 wt%; SD = 0.33; Table T12; Fig. F12B). The sharp decline in TOC in the upper two cores is characteristic of oxidation and microbial diagenesis of organic matter (OM). Calculated C/N ratios similarly decrease downhole from 5 to 8 above 40 mcd to unreasonably low values (Table T12; Fig. F12C), indicating nitrogen presence in clay matrices (see “Organic Geochemistry,” p. 11, in the “Site 1145” chapter). We conclude that the low levels of OM in these sediments are dominated by degraded marine matter.

INORGANIC GEOCHEMISTRY

Inorganic chemical analyses were conducted on seven interstitial water samples from Hole 1147A squeezed from whole-round samples at a frequency of one per core in the first five cores and one every second core thereafter. Analytical methods are detailed in “Inorganic Geochemistry,” p. 17, in the “Explanatory Notes” chapter. The concentrations of dissolved interstitial constituents are presented in Table T13, and the profiles with depth are shown in Figure F13. This short interval was drilled to recover a recent sedimentary section thought to be missing at Site 1148, and as such it yields an abbreviated picture of sediment water interactions. The primary interstitial water variations observed at this site are those mediated by sulfate reduction of organic matter.

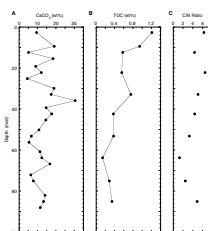
F11. Age-depth model, LSR, and MAR, p. 21.



T11. Sedimentation and accumulation rates for selected intervals, p. 41.

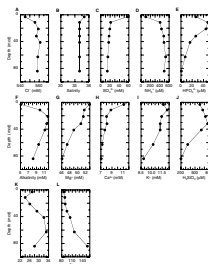
T12. IC, CaCO₃, TC, TOC, TN, and TS contents, p. 42.

F12. CaCO₃, TOC, and organic C/N ratio vs. depth, p. 22.



T13. Interstitial water composition, p. 43.

F13. Interstitial water measurements, p. 23.



Longer term reactions, such as clay alteration and diagenesis of biogenic sediments, were not well expressed in the nine cores recovered at this site.

Chloride and Salinity

Chloride (Cl^-) concentrations in interstitial waters at Site 1147 increase from 545 mM near the surface to 559 mM at 19 mcd and are relatively constant below this depth (Fig. F13A; Table T13). Interstitial water salinities decrease from 35 to 34 between 3 and 10 mcd and then are constant below this depth (Fig. F13B; Table T13).

Sulfate, Ammonium, Phosphate, Alkalinity, and pH

Sulfate decreases from 26.6 mM in the first core to 21.2 mM by the second core and is relatively constant below this depth, 17.3 ± 2.6 mM (Fig. F13C; Table T13), indicating that sulfate reduction is incomplete at this site. Ammonium (NH_4^+) increases between the first and second core as well and then increases slightly downhole (Fig. F13D; Table T13). Dissolved phosphate (HPO_4^{2-}) concentrations increase to a maximum of 47.7 mM in the zone of sulfate reduction and then decrease rapidly to reach near-zero values by 84 mcd (Fig. F13E; Table T13). Alkalinity increases to a maximum of 11.8 mM by the third core, then decreases downhole (Fig. F13F; Table T13). A minimum in pH is centered at the depth of the maximum in NH_4^+ , HPO_4^{2-} , and alkalinity (Table T13). Incomplete sulfate reduction and relatively constant or decreasing concentrations of methanogenic products NH_4^+ , HPO_4^{2-} , and alkalinity below the zone of sulfate reduction are consistent with the low methane values at this site, indicating that methanogenesis is not an active process in these sediments.

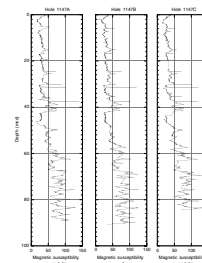
Potassium, Magnesium, and Calcium

Magnesium (Mg^{2+}) concentrations decrease with depth from 52.9 mM at the top to a minimum of ~46.1 mM at the bottom of the hole (Fig. F13G; Table T13). Dissolved calcium concentrations (Ca^{2+}) decrease rapidly in the zone of sulfate reduction from a maximum of 11.1 mM in the first core to 8.0 mM by the third core, presumably reflecting the removal of Ca^{2+} through inorganic calcite precipitation, and then decrease very slightly toward the base of the hole (Fig. F13H; Table T13). Dissolved potassium (K^+) concentrations decrease downhole from ~11.7 mM near the surface to 8.9 mM at the base of the hole (Fig. F13I; Table T13). Changes in all three of these elements are very similar to the corresponding profiles at Site 1146 over the same ~80-m depth interval, suggesting that similar processes of clay and volcanic ash alteration are at work deeper at this site.

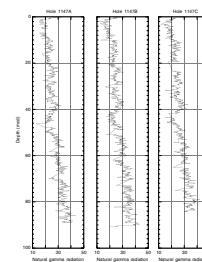
Silica, Lithium, and Strontium

Dissolved silica (H_4SiO_4) concentrations increase to a maximum of 769 mM at 32 mcd and then decrease below this depth (Fig. F13J; Table T13). Lithium (Li^+) decreases between the first and second core to reach a minimum of 24 mM, increases to a maximum of 33 mM at 84 mcd, and then decreases downhole (Fig. F13K; Table T13). Dissolved strontium concentrations (Sr^{2+}) increase downhole from a minimum at the

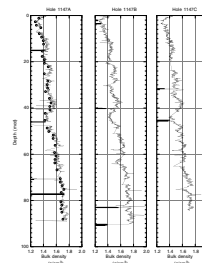
F14. Magnetic susceptibility measurements, p. 24.



F15. Natural gamma radiation measurements, p. 25.



F16. Bulk density measurements from GRA and MAD methods, p. 26.



surface of 86 mM to a maximum of 153 mM at the base of the hole (Fig. F13L; Table T13). Changes in Li and Sr with depth at Site 1147 are relatively small, reflecting the small changes in diagenesis of biogenic sediments in the upper sediments.

PHYSICAL PROPERTIES

Sampling

At Site 1147, physical properties were measured on whole-round sections, split-core sections, and discrete samples from the latter. Whole-round core logging with the MST included GRA bulk density, MS, NGR, and *P*-wave velocity logging on all cores. Sampling intervals were 5 cm for all cores in the three holes. The *P*-wave logger (PWL) data were bad because of instrument problems and/or cracks or voids in the sediment cores. The PWL data are not shown in this report but are available from the Ocean Drilling Program JANUS database (see the “[Related Leg Data](#)” contents list). One thermal conductivity measurement per core was also performed on the whole-round sections. Color spectral reflectance was measured on the archive halves of all split cores at 4-cm intervals. Moisture, density and *P*-wave velocity were measured on discrete samples from split-core sections at intervals of one measurement per section (1.5 m) (see “[Physical Properties](#),” p. 18, in the “[Explanatory Notes](#)” chapter).

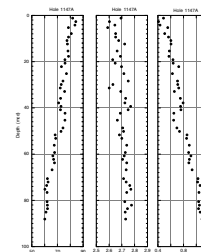
Results

Core physical properties measurements at Site 1147 display two distinct intervals: the upper interval, from 0 to 42 mcd; and the lower interval, from 42 mcd to the bottom of the hole (91 mcd). The transition between the two intervals is characterized by an apparent discontinuity in the general trend of all data sets. Data from MS, GRA, and NGR all show a gently increasing general trend, whereas porosity, which decreases in the upper interval, is sharply offset at 42 mcd and then continues to decrease below that depth (Figs. F14, F15, F16, F17). The CSR values show a gently increasing trend from 37% to 43% in the upper interval and level off, varying around 43% below that depth (Fig. F18). *P*-wave velocities decline very gently from ~1493 to ~1487 m/s in the top 42 mcd and increase steadily to ~1520 m/s in the lower interval (Fig. F19). Grain density reveals significantly more scatter in the upper interval than below 42 mcd, superimposed on the general trend offset and indicating a greater degree of mineralogic variability (Fig. F17).

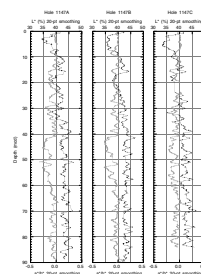
The general trends in the core-logging data (Figs. F14, F15, F16) and CSR (Fig. F18) are superimposed by large-amplitude cyclic fluctuations over the entire interval. These fluctuations are interpreted as glacial-interglacial compositional changes.

In Hole 1147C, the core temperature equilibration times were recorded for Cores 184-1147C-1H through 7H (Fig. F20). This test suggested that the cores need 5 hr to equilibrate to room temperature. For practical reasons, complete equilibration could not be achieved. A time of 2–3 hr was deemed reasonable according to the measurements because then the gradient of most equilibration curves becomes very small, and the difference between core temperature and ambient temperature in the core lab is negligible.

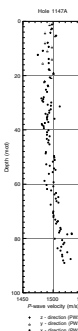
F17. Porosity, grain density, and dry density for Hole 1147A, p. 27.



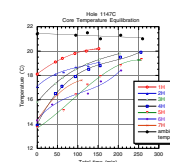
F18. Color spectral reflectance measurements, p. 28.



F19. *P*-wave velocity measurements for Hole 1147A, p. 29.



F20. Partial core temperature equilibration curves for Cores 184-1147C-1H through 7H, p. 30.



REFERENCES

- Blow, W.H., 1969. Late middle Eocene to Recent planktonic foraminiferal biostratigraphy. In Brönnimann, P., and Renz, H.H. (Eds.), *Proc. First Int. Conf. Planktonic Microfossils, Geneva, 1967*: Leiden (E.J. Brill), 1:199–422.
- Li, B., 1997. Paleooceanography of the Nansha Area, southern South China Sea since the last 700,000 years [Ph.D. dissert.]. Nanjing Inst. Geol. Paleontol., Academia Sinica, Nanjing, China. (in Chinese, with English abstract)
- Schönfeld, J., 1996. The “*Stilostomella* Extinction”: structure and dynamics of the last turnover in deep-sea benthic foraminiferal assemblages. In Mogurlevsky, A., and Whatly, R. (Eds.), *Microfossils and Oceanic Environments*: Aberystwyth (Univ. Wales, Aberystwyth Press), 27–37.
- Thompson, P.R., Bé, A.W.H., Duplessy, J.-C., and Shackleton, N.J., 1979. Disappearance of pink-pigmented *Globigerinoides ruber* at 120,000 yr BP in the Indian and Pacific oceans. *Nature*, 280:554–558.

Figure F1. Smoothed (11-point running average)/correlated MS data and the splice for the three holes at Site 1147 (spliced MS data for this figure are also available in [ASCII format](#)). The order of the four arrays (the splice and Holes 1147A through 1147C) increases outward from the origin. The hole arrays are offset from each other—and from the splice—by a constant (10.0×10^{-5} SI units) so that only the splice is plotted relative to the absolute MS value. Lines identify the splice tie points.

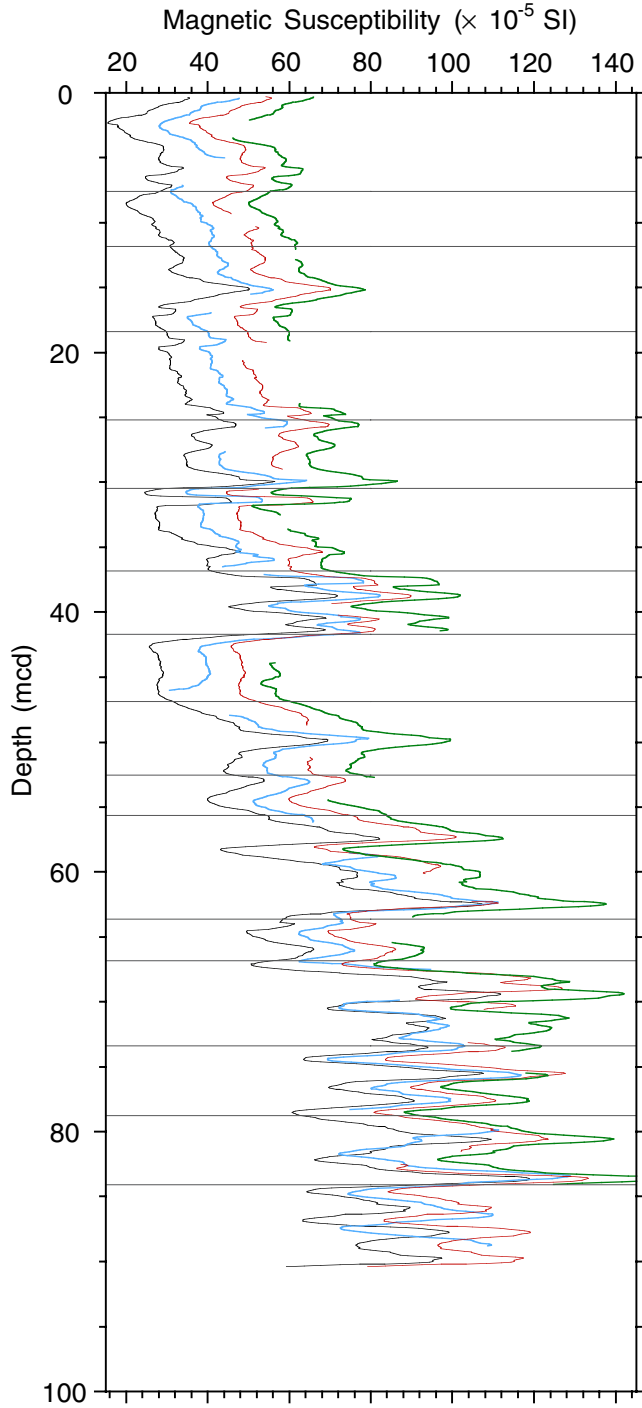


Figure F2. Smoothed (11-point running average)/correlated NGR data and the splice for the three holes at Site 1147 (spliced NGR data for this figure are also available in [ASCII format](#)). The order of the four arrays (the splice and Holes 1147A through 1147C) increases outward from the origin. The hole arrays are offset from each other—and from the splice—by a constant (9 cps) so that only the splice is plotted relative to the absolute NGR value. Lines identify the splice tie points.

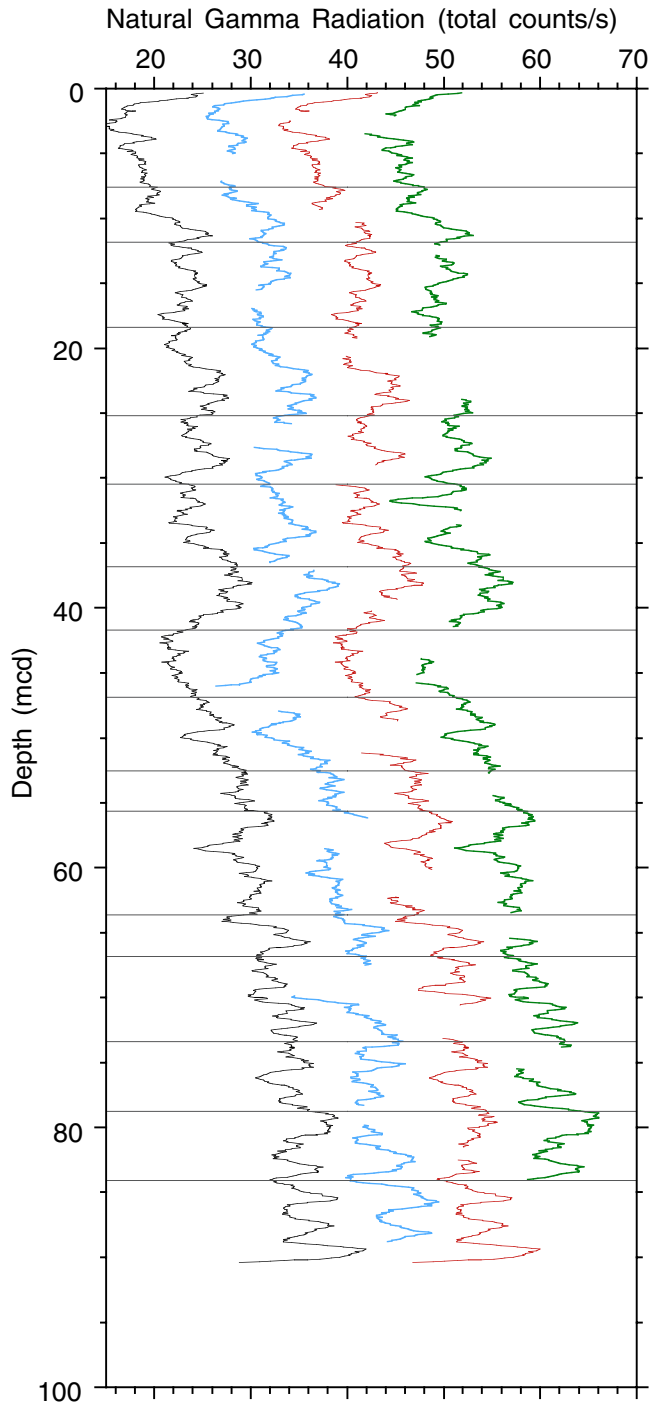


Figure F3. Smoothed (11-point running average)/correlated GRA data and the splice for the three holes at Site 1147 (spliced GRA data for this figure are also available in [ASCII format](#)). The order of the four arrays (the splice and Holes 1147A through 1147C) increases outward from the origin. The hole arrays are offset from each other—and from the splice—by a constant (0.15 g/cm^3) so that only the splice is plotted relative to the absolute GRA value. Values ≤ 1.03 and $\geq 2.4 \text{ (g/cm}^3\text{)}$ have been culled. Lines identify the splice tie points.

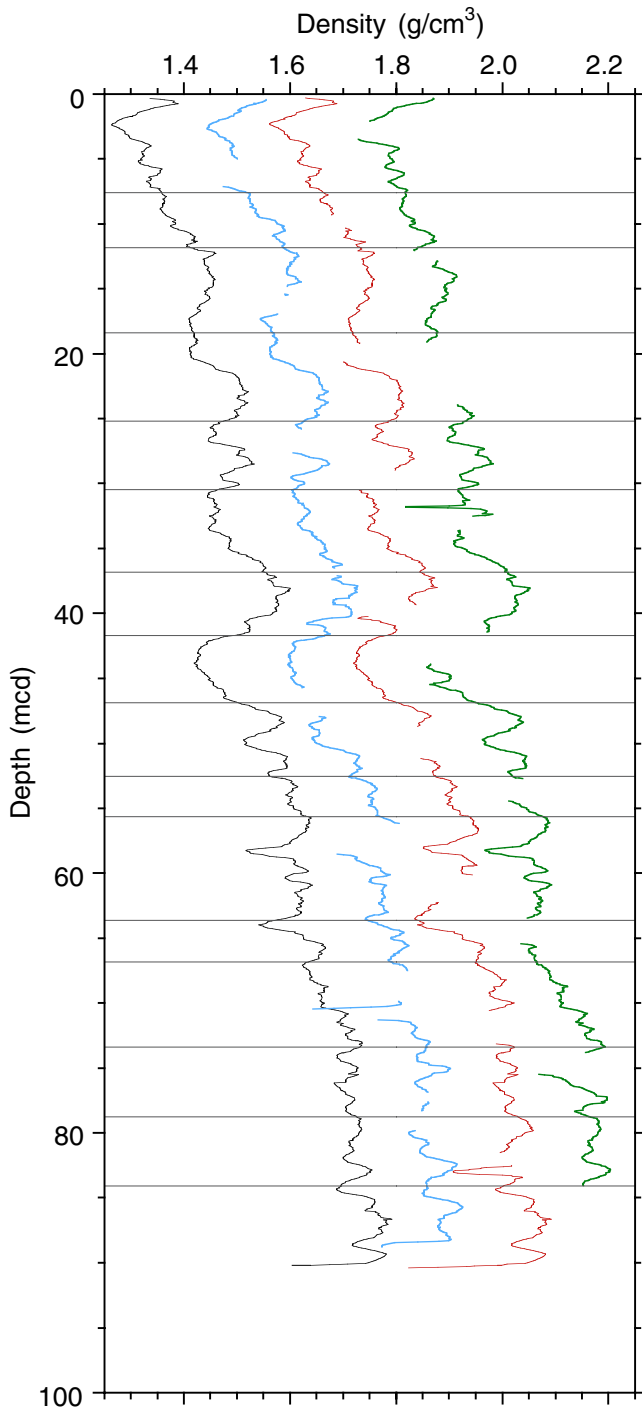


Figure F4. Smoothed (11-point running average)/correlated L^* (“lightness”) values from the CSR data and the splice for the three holes at Site 1147 (spliced CSR data for this figure are also available in [ASCII format](#)). The order of the four arrays (the splice and Holes 1147A through 1147C) increases outward from the origin. The hole arrays are offset from each other—and from the splice—by a constant (8%) so that only the splice is plotted relative to the absolute L^* value. Values $\leq 1\%$ have been culled. Lines identify the splice tie points.

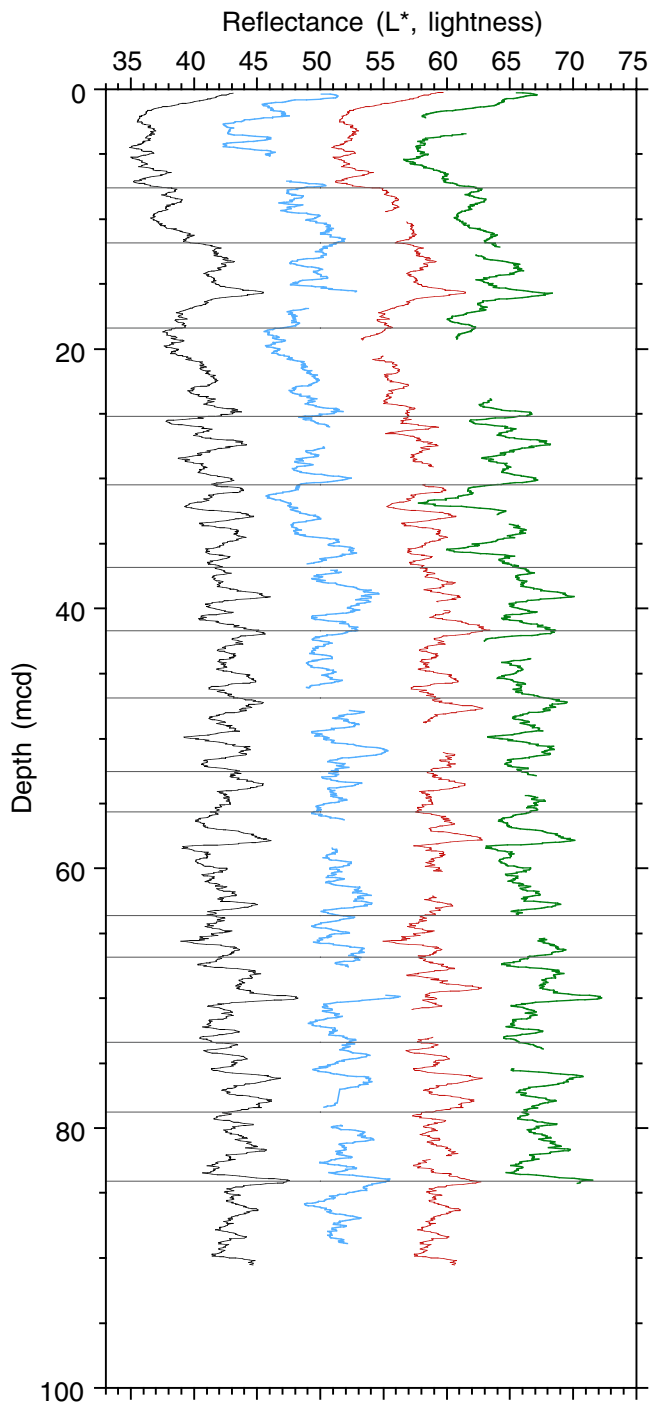


Figure F5. Summary of the recovered section at Site 1147, showing lithologic unit, sediment types, lightness intensity (L^* parameter) and the a^* parameter, occurrence of “iron sulfide,” pyrite, and green layers. High positive values of a^* correspond to high red intensity, whereas high negative values correspond to high green intensity. L^* and a^* values correspond to measurements made from Hole 1147B. Occurrences of “iron sulfide,” pyrite, and green layers are core-averaged occurrences per meter from Hole 1147A.

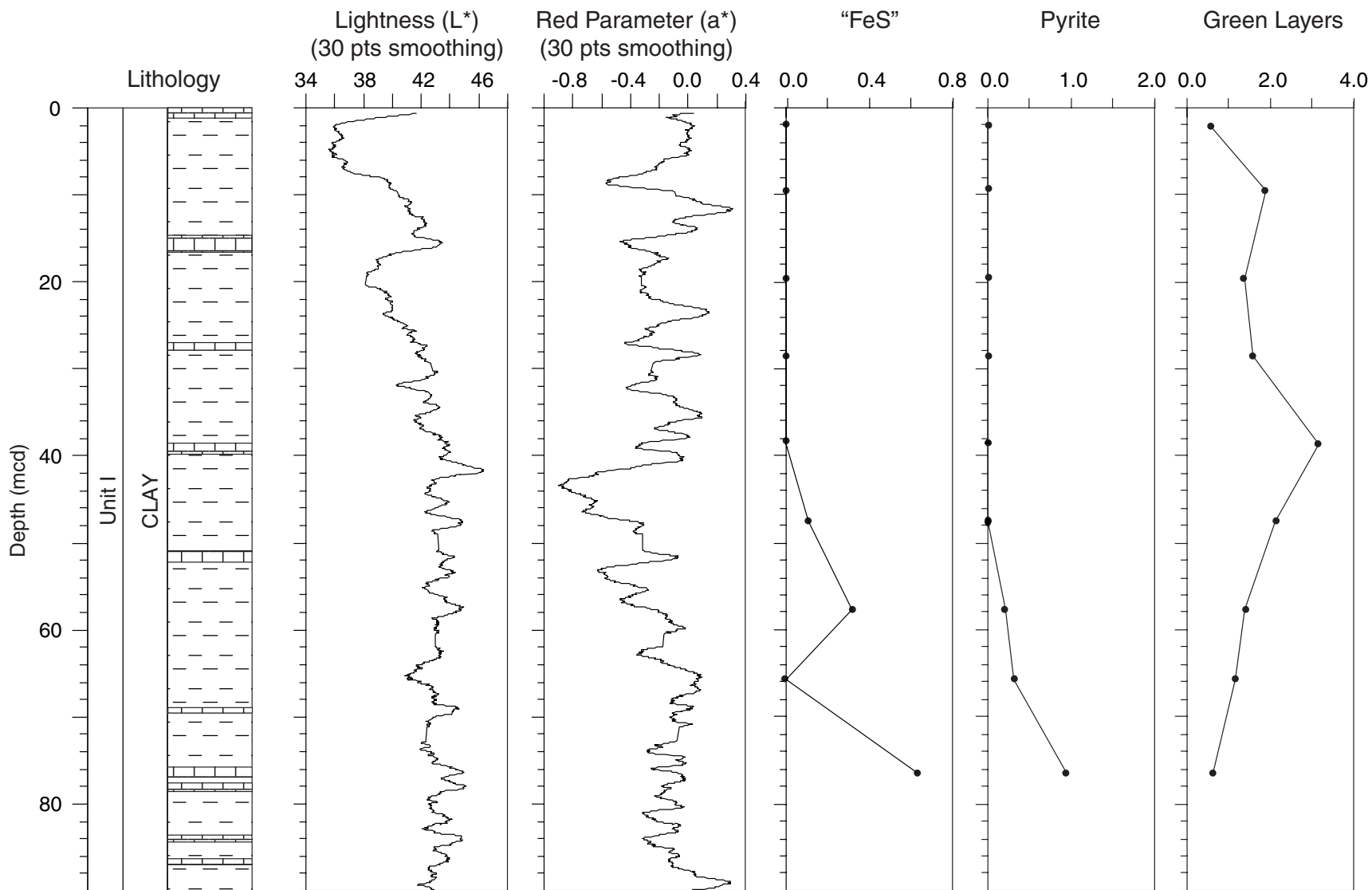


Figure F6. Calcareous nannofossil and planktonic foraminifer preservation and nannofossil abundance for Hole 1147A. P = poor, M = moderate, G = good, VG = very good, R = rare, F = few, C = common, A = abundant.

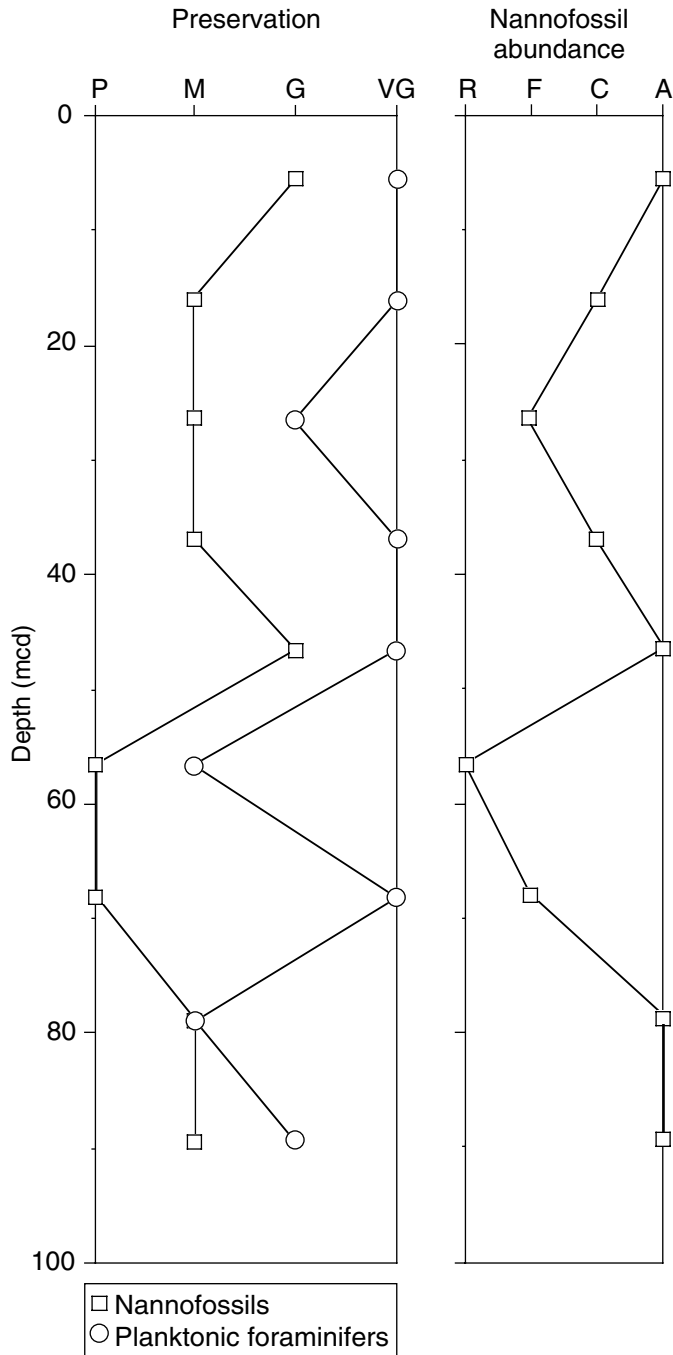


Figure F7. Age-depth plot at Hole 1147A. All biostratigraphic events are listed in Table T7, p. 37. The average sedimentation rate is calculated based on two control points (control points are marked by * in Table T7, p. 37).

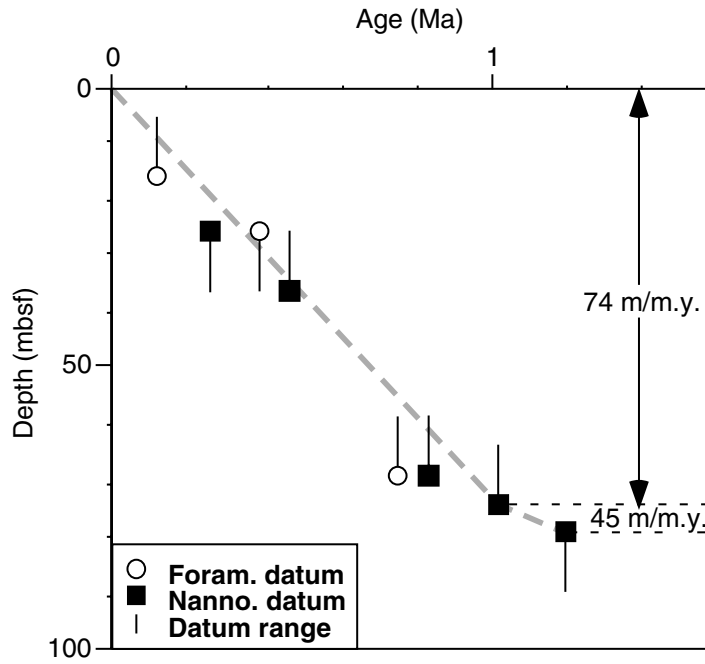


Figure F8. Declination and inclination for Hole 1147A, 0–88.5 mcd, obtained from long-core measurements (Cores 184-1147A-1H and 2H are not oriented).

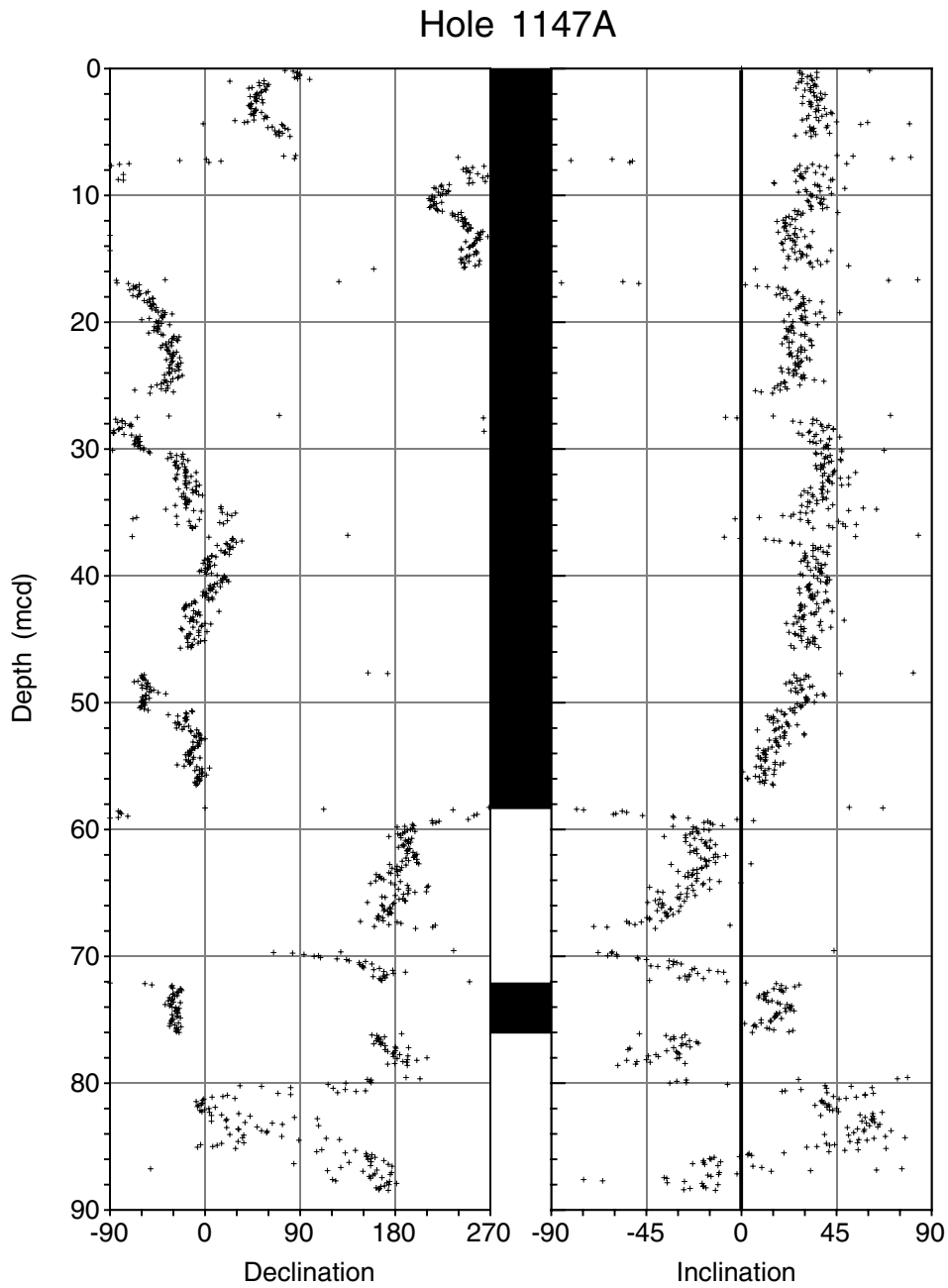


Figure F9. Declination and inclination for Hole 1147B (Cores 184-1147B-1H and 2H are not oriented).

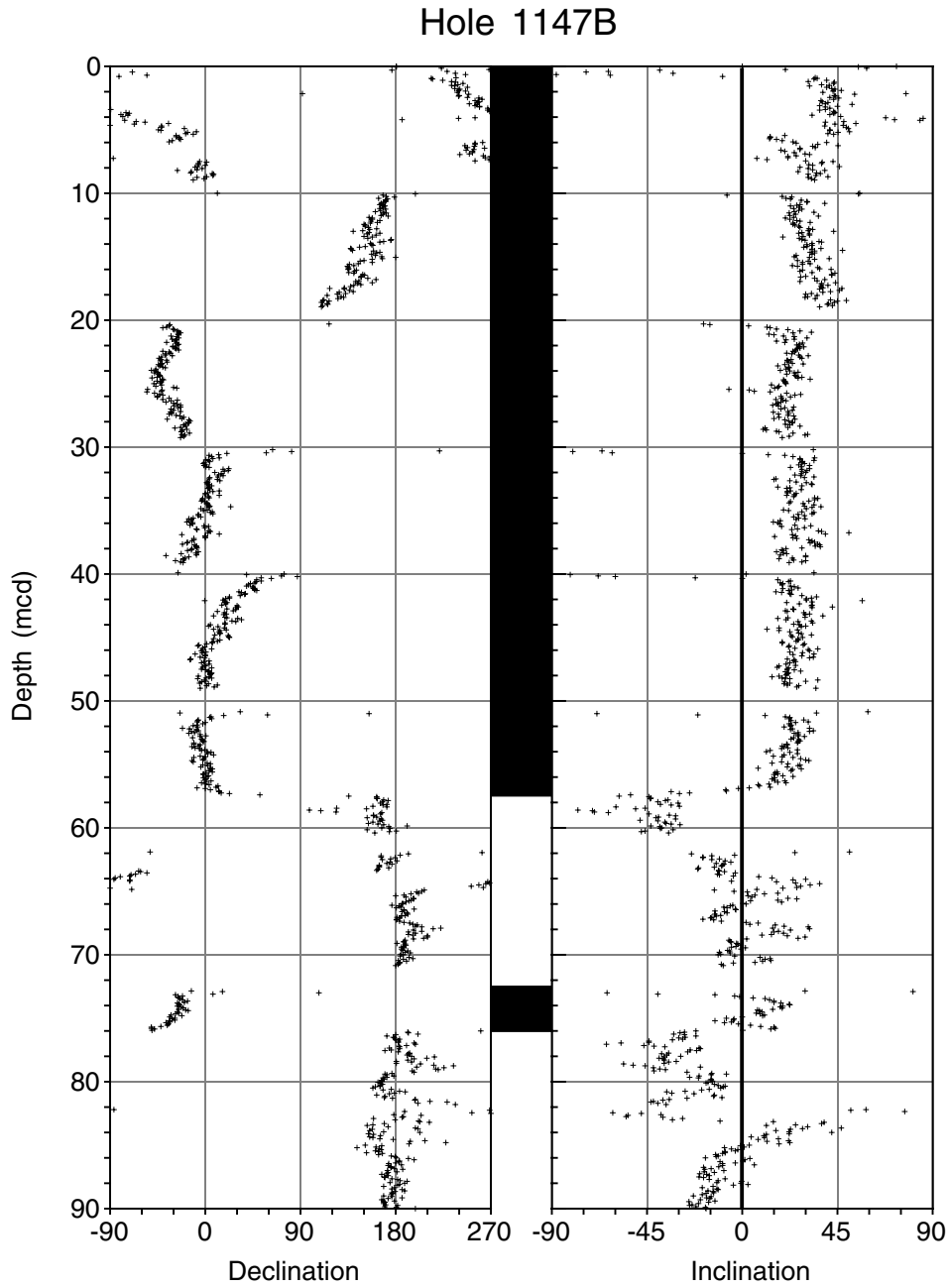


Figure F10. Declination and inclination for Hole 1147C (Cores 184-1147C-1H and 2H are not oriented).

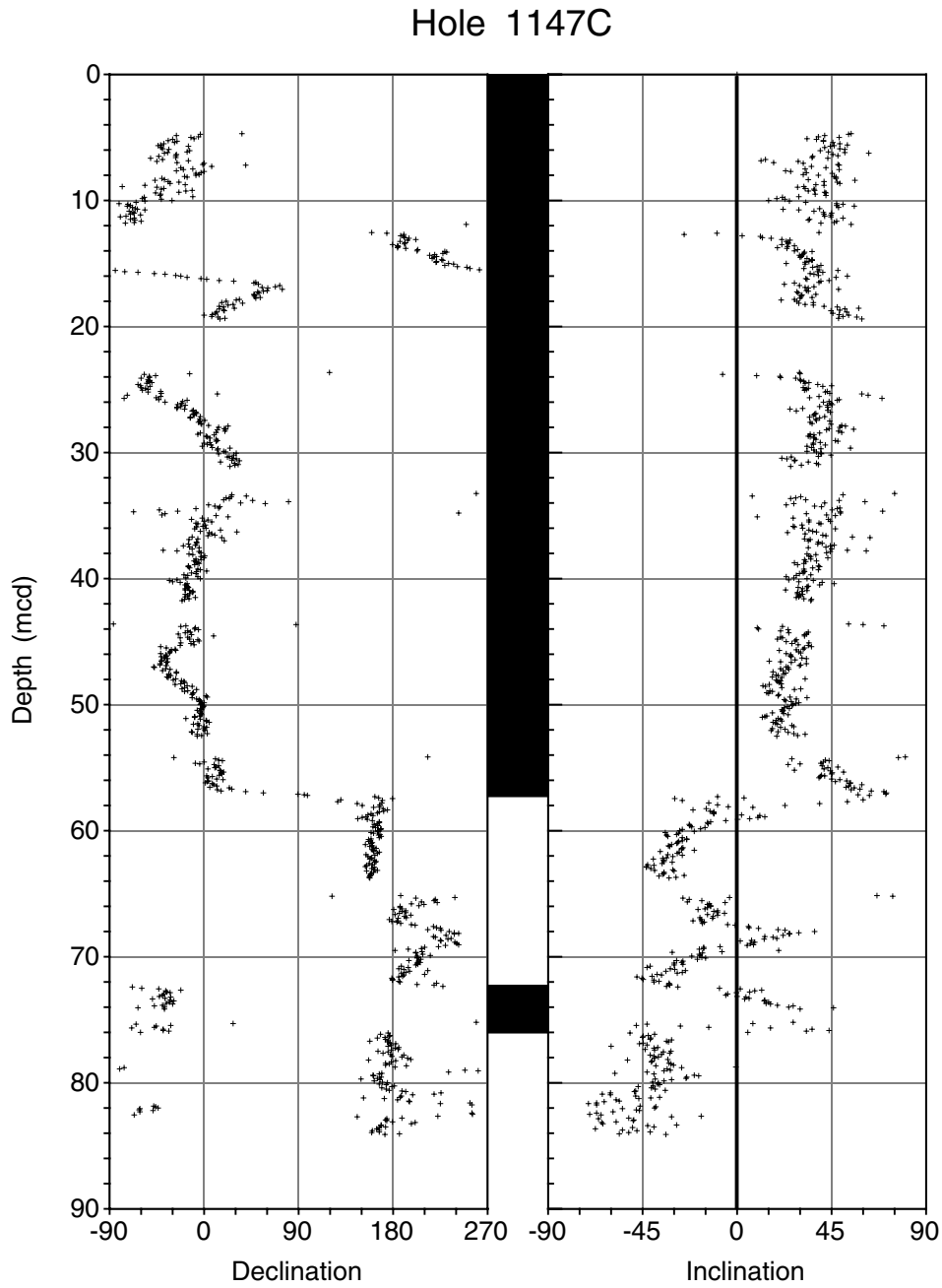


Figure F11. (A) Age-depth model, (B) linear sedimentation rates (LSR) and mass accumulation rates (MAR) vs. depth, and (C) LSR and MAR vs. age for Site 1147. Construction of model rates, LSR, and MAR is explained in **“Sedimentation and Accumulation Rates,”** p. 13, in the “Explanatory Notes” chapter. In (A), diamonds = calcareous nannofossils, circles = foraminifers, squares = paleomagnetic reversals; in (B) and (C), solid lines = total sediment LSR, dashed lines = carbonate LSR, stippled columns = total sediment MAR, solid columns = carbonate MAR. B/M = Brunhes/Matuyama.

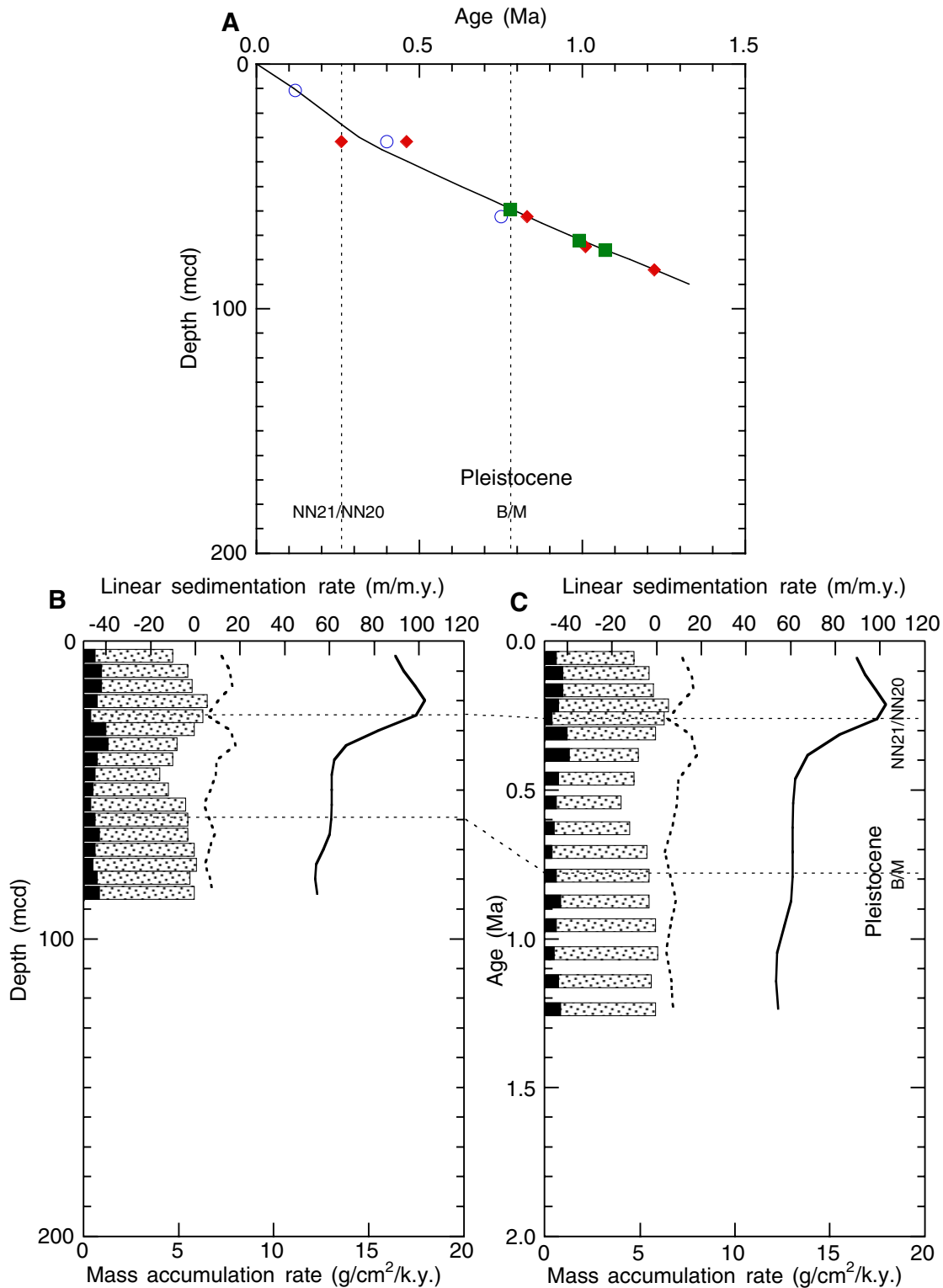


Figure F12. (A) Carbonate, (B) total organic carbon, and (C) organic C/N ratio at Site 1147 vs. depth (Hole 1147A).

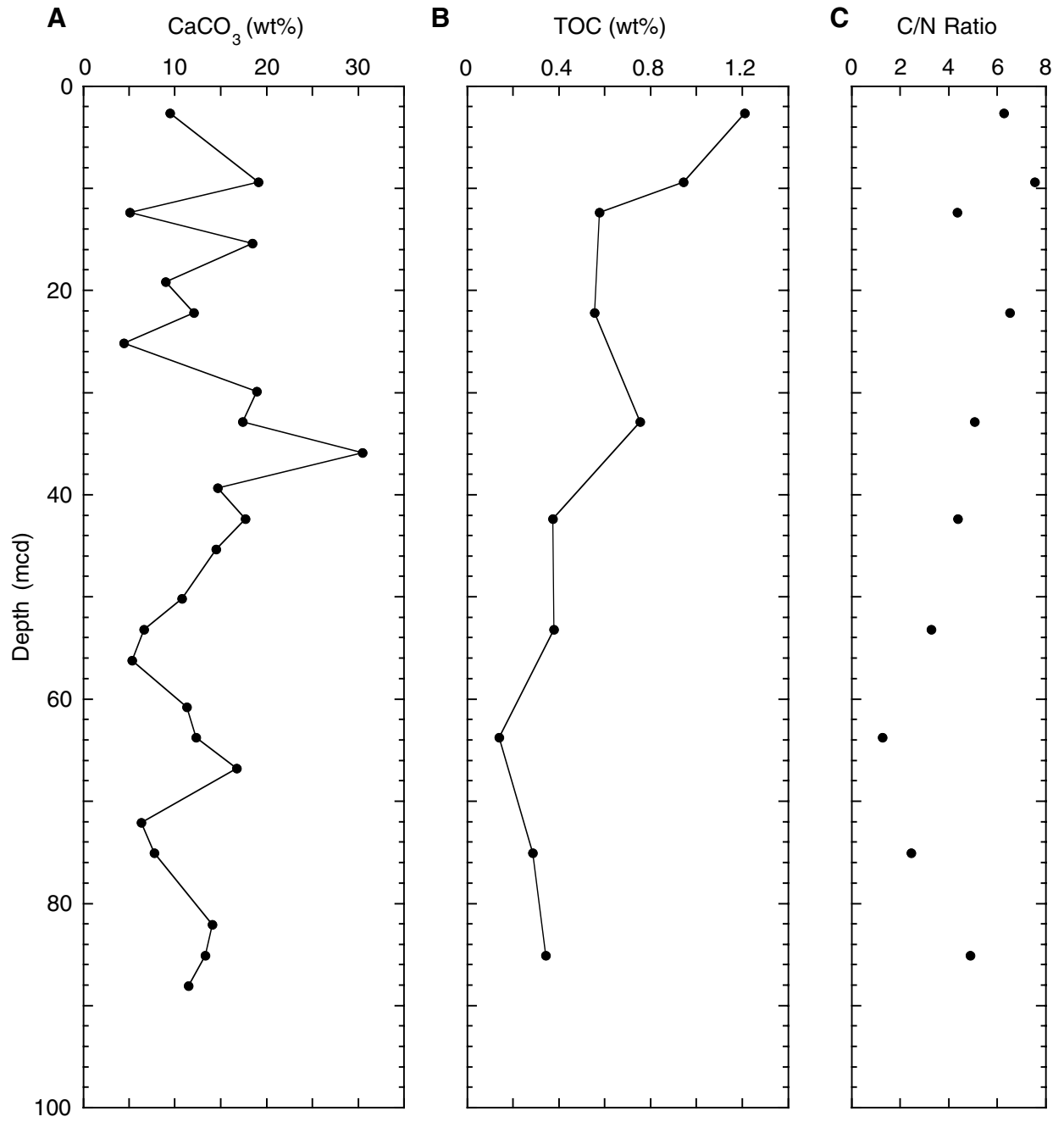


Figure F14. Magnetic susceptibility measurements at Site 1147 plotted for each hole.

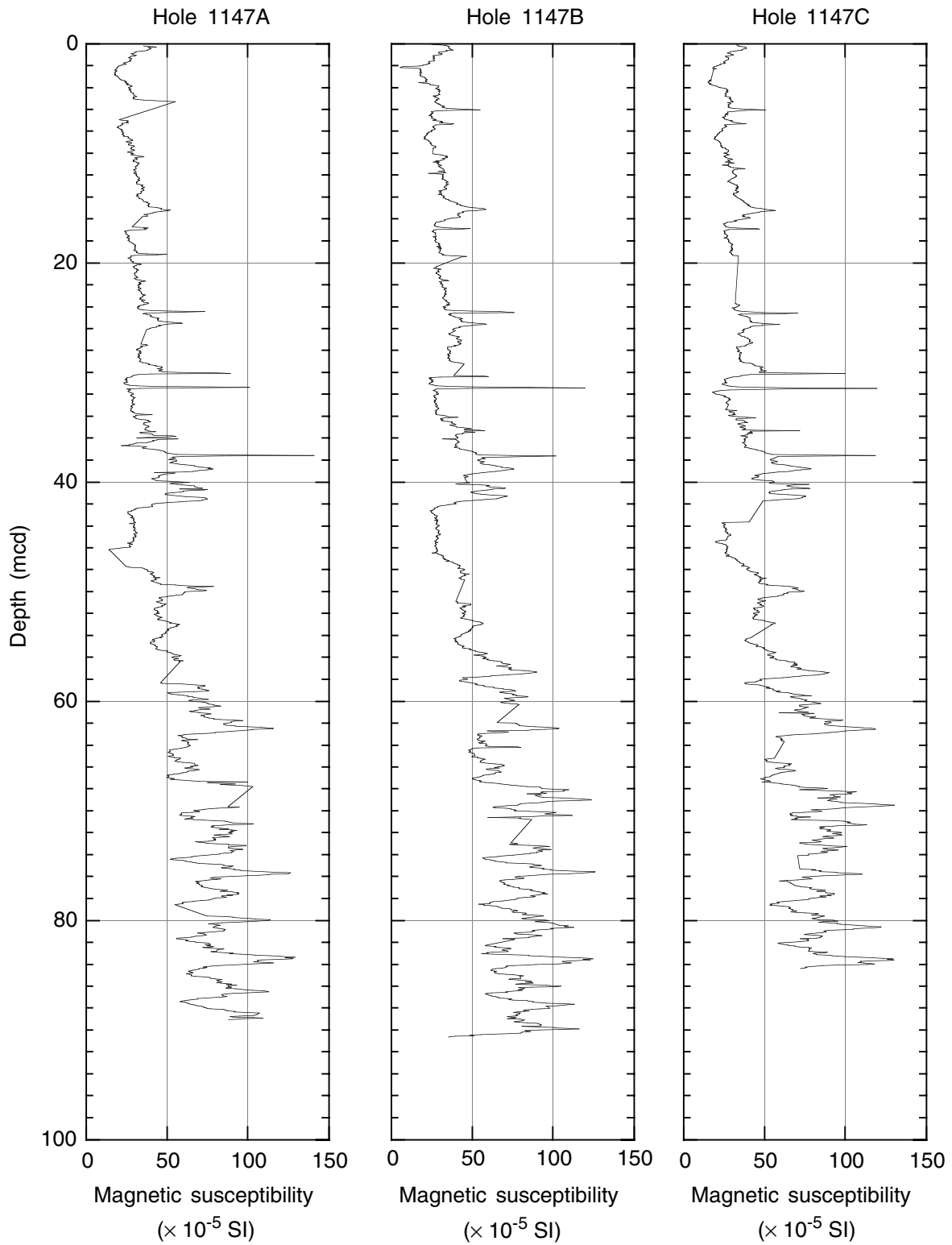


Figure F15. Natural gamma radiation measurements at Site 1147 plotted for each hole.

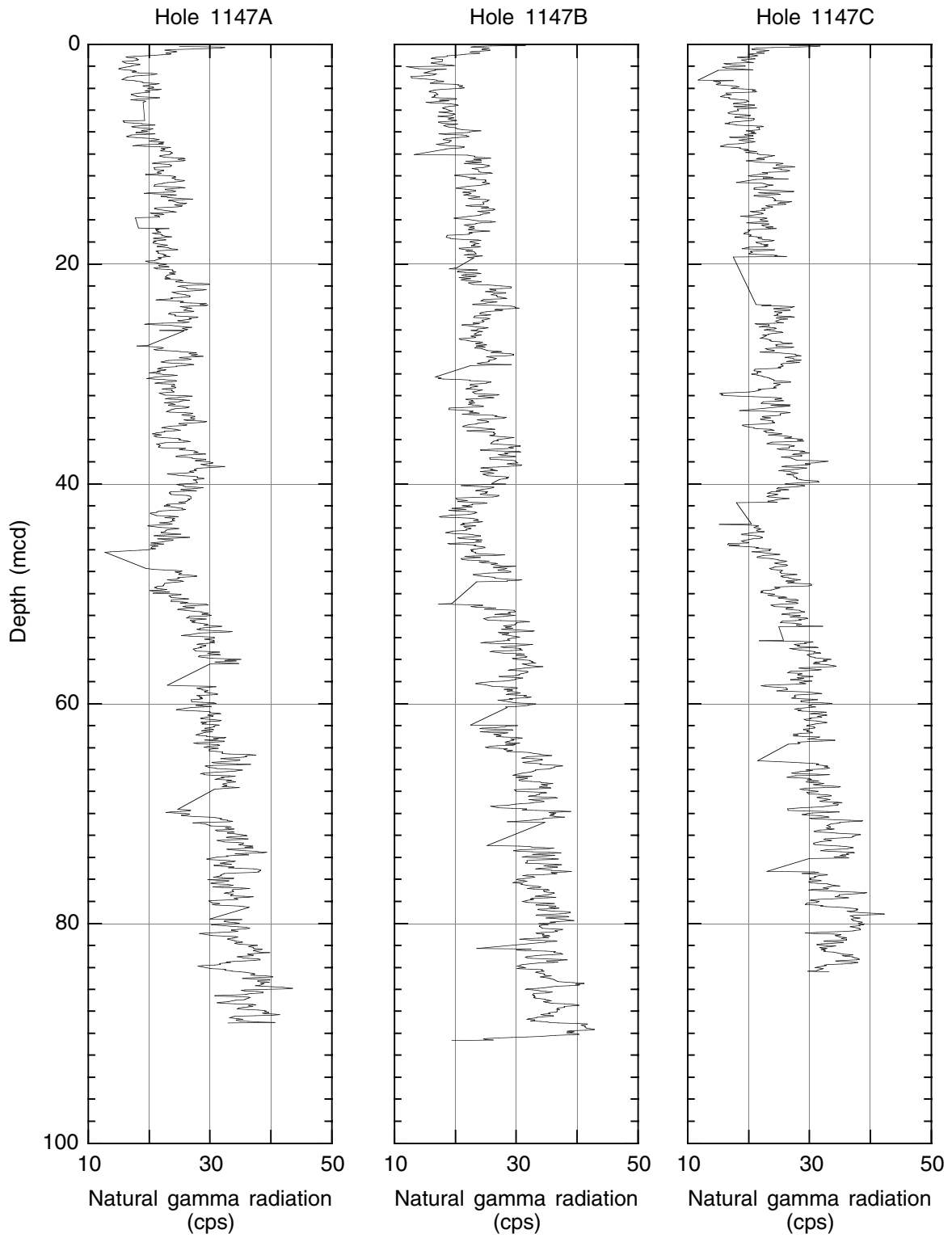


Figure F16. Bulk density measurements from GRA (line) and moisture and density (MAD) methods (open circles) at Site 1147 plotted for each hole.

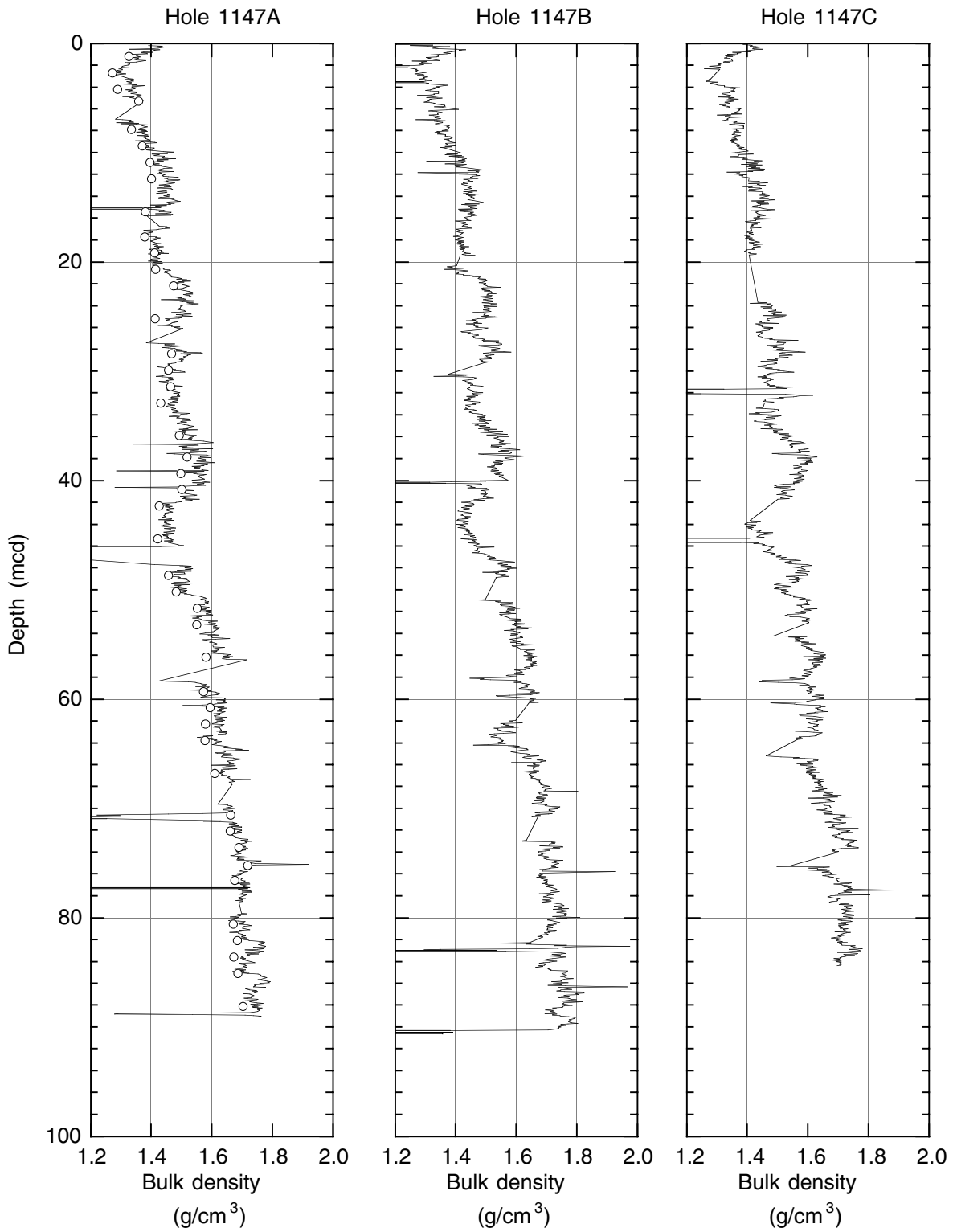


Figure F17. Porosity, grain density, and dry density from MAD measurements for Hole 1147A.

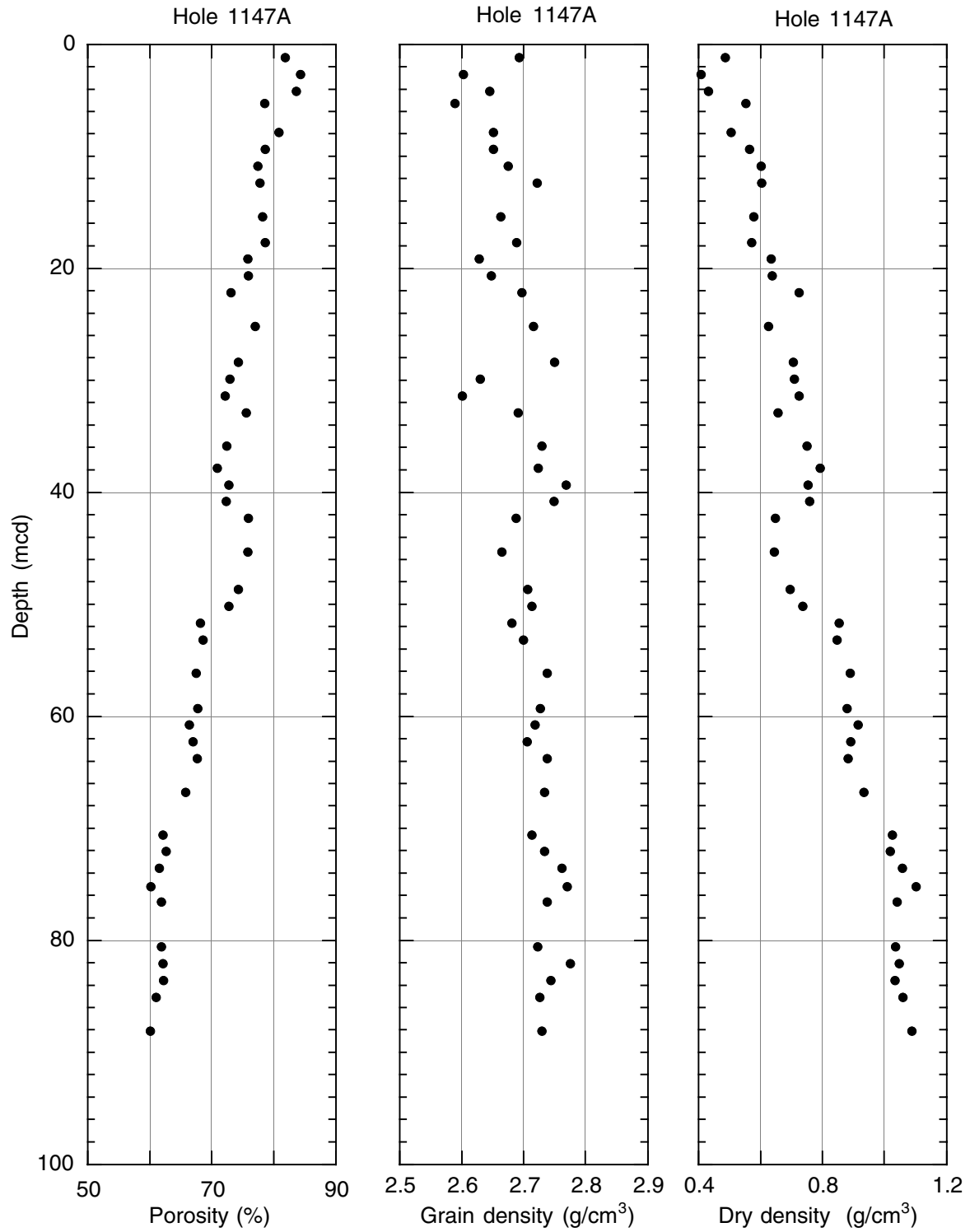


Figure F18. Color spectral reflectance measurements from split-core surfaces at Site 1147 plotted for each hole. L^* , a^* , and b^* are standard parameters calculated by the Minolta CM-2002 photospectrometer from the spectral data. L^* = black line, a^*/b^* = gray line.

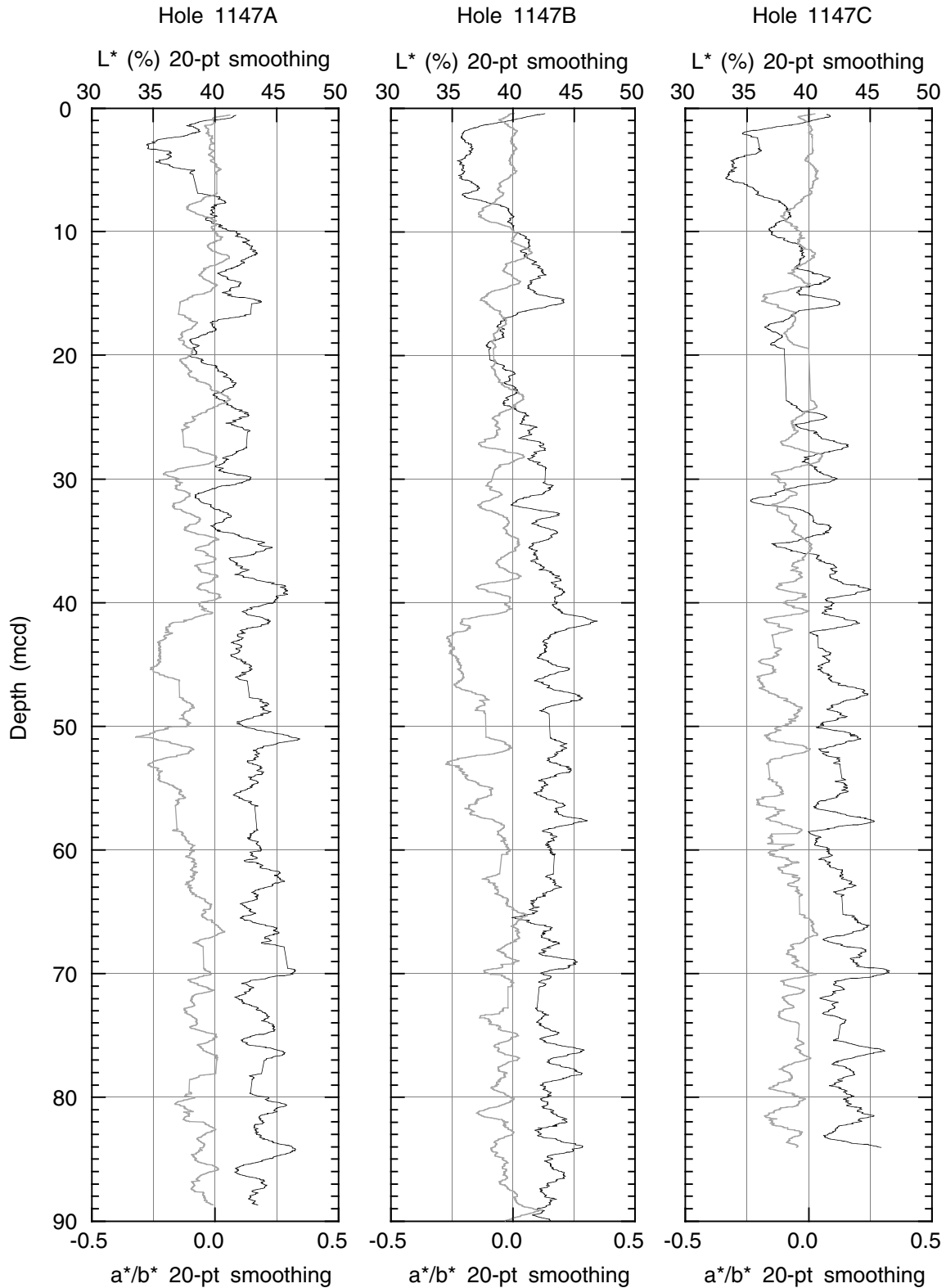


Figure F19. *P*-wave velocity measurements for Hole 1147A. For a discussion of directional components, see “Physical Properties,” p. 18, in the “Explanatory Notes” chapter.

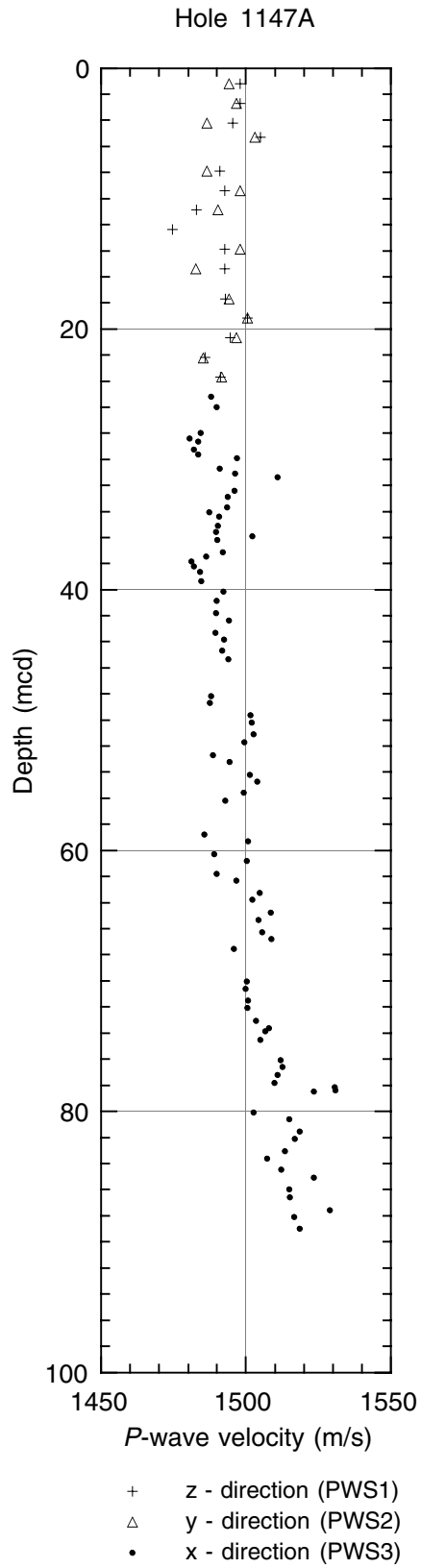


Figure F20. Partial core temperature equilibration curves for Cores 184-1147C-1H through 7H.

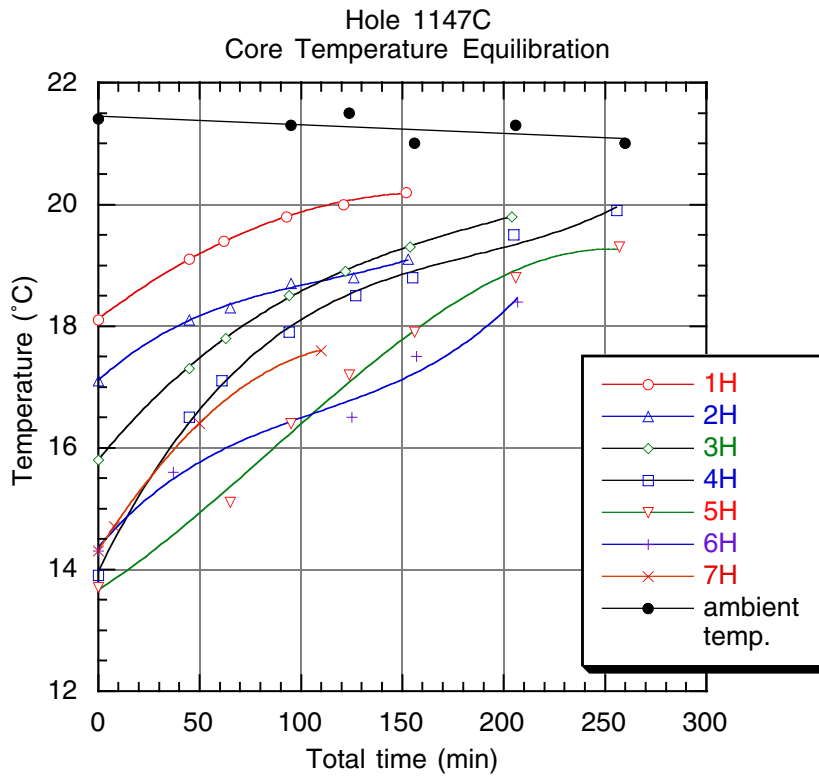


Table T1. Site 1147 coring summary.

Core	Date (March 1999)	Time (UTC + 8 hr)	Depth			Length (m)		Recovery (%)
			Top (mbsf)	Bottom (mbsf)	Top (mcd)	Cored	Recovered	
184-1147A-								
1H	29	1835	0.0	5.4	0.15	5.4	5.33	98.7
2H	29	1930	5.4	14.9	6.85	9.5	9.16	96.4
3H	29	2020	14.9	24.4	16.65	9.5	9.80	103.2
4H	29	2110	24.4	33.9	27.35	9.5	9.63	101.4
5H	29	2200	33.9	43.4	36.80	9.5	9.81	103.3
6H	29	2300	43.4	52.9	47.65	9.5	8.95	94.2
7H	29	2350	52.9	62.4	58.25	9.5	9.84	103.6
8H	30	0040	62.4	71.9	69.55	9.5	9.32	98.1
9H	30	0125	71.9	81.4	79.55	9.5	9.87	103.9
Totals:						81.4	81.71	100.4
184-1147B-								
1H	30	0315	0.0	9.5	0.00	9.5	9.79	103.1
2H	30	0350	9.5	19.0	10.00	9.5	9.70	102.1
3H	30	0445	19.0	28.5	20.30	9.5	9.20	96.8
4H	30	0535	28.5	38.0	30.20	9.5	9.77	102.8
5H	30	0620	38.0	47.5	39.90	9.5	9.32	98.1
6H	30	0705	47.5	57.0	50.85	9.5	9.83	103.5
7H	30	0755	57.0	66.5	61.90	9.5	9.33	98.2
8H	30	0835	66.5	76.0	72.70	9.5	9.92	104.4
9H	30	0925	76.0	85.5	82.20	9.5	8.63	90.8
Totals:						85.5	85.49	100.0
184-1147C-								
1H	30	1100	0.0	2.6	0.05	2.6	2.58	99.2
2H	30	1150	2.6	12.1	3.20	9.5	9.38	98.7
3H	30	1235	12.1	21.6	12.55	9.5	7.16	75.4
4H	30	1320	21.6	31.1	23.65	9.5	9.52	100.2
5H	30	1410	31.1	40.6	33.28	9.5	9.71	102.2
6H	30	1505	40.6	50.1	43.60	9.5	9.58	100.8
7H	30	1555	50.1	59.6	54.15	9.5	9.92	104.4
8H	30	1640	59.6	69.1	65.15	9.5	9.22	97.1
9H	30	1730	69.1	78.6	75.20	9.5	9.57	100.7
Totals:						78.6	76.64	97.5

Notes: UTC = Universal Time Coordinated. This table is also available in [ASCII format](#).

Table T2. Site 1147 coring summary by section.

Core	Date (March 1999)	Time (UTC + 8 hr)	Core depth (mbsf)		Length (m)		Recovery (%)	Section	Length (m)		Section depth (mbsf)		Top depth (mcd)	Catwalk samples	Comments
			Top	Bottom	Cored	Recovered			Liner	Curated	Top	Bottom			
184-1147A- 1H	29	1835	0.0	5.4	5.4	5.33	98.7								
								1	1.50	1.50	0.00	1.50	0.15		
								2	1.50	1.50	1.50	3.00	1.65	IW	
								3	1.50	1.50	3.00	4.50	3.15	HS	
								4	0.73	0.73	4.50	5.23	4.65		
								CC(NS)	0.10	0.10	5.23	5.33	5.38	PAL	All to PAL
Totals:									5.33	5.33					
2H	29	1930	5.4	14.9	9.5	9.16	96.4								
								1	1.50	1.50	5.40	6.90	6.85		
								2	1.50	1.50	6.90	8.40	8.35		
								3	1.50	1.50	8.40	9.90	9.85	IW	
								4	1.50	1.50	9.90	11.40	11.35	HS	
								5	1.50	1.50	11.40	12.90	12.85		
6	1.51	1.51	12.90	14.41	14.35										
CC(w/CC)	0.15	0.15	14.41	14.56	15.86	PAL									
Totals:									9.16	9.16					
3H	29	2020	14.9	24.4	9.5	9.80	103.2								
								1	1.50	1.50	14.90	16.40	16.65		
								2	1.50	1.50	16.40	17.90	18.15		
								3	1.50	1.50	17.90	19.40	19.65	IW	
								4	1.50	1.50	19.40	20.90	21.15	HS	
								5	1.50	1.50	20.90	22.40	22.65		
6	1.50	1.50	22.40	23.90	24.15										
7	0.58	0.58	23.90	24.48	25.65										
CC(w/7)	0.22	0.22	24.48	24.70	26.23	PAL									
Totals:									9.80	9.80					Oriented
4H	29	2110	24.4	33.9	9.5	9.63	101.4								
								1	1.50	1.50	24.40	25.90	27.35		
								2	1.50	1.50	25.90	27.40	28.85		
								3	1.50	1.50	27.40	28.90	30.35	IW	
								4	1.50	1.50	28.90	30.40	31.85	HS	
								5	1.50	1.50	30.40	31.90	33.35		
6	1.50	1.50	31.90	33.40	34.85										
7	0.49	0.49	33.40	33.89	36.35										
CC(w/7)	0.14	0.14	33.89	34.03	36.84	PAL	Dimpled, cut off-line from normal								
Totals:									9.63	9.63					Oriented
5H	29	2200	33.9	43.4	9.5	9.81	103.3								
								1	1.50	1.50	33.90	35.40	36.80		
								2	1.50	1.50	35.40	36.90	38.30		
								3	1.50	1.50	36.90	38.40	39.80	IW	
4	1.50	1.50	38.40	39.90	41.30	HS									

Notes: UTC = Universal Time Coordinated. The notation "CC (w/x)" refers to the D-tube in which the core catcher is stored, where x is the section number (1–8 or CC). NS = no section, IW = interstitial waters, PAL = paleontology, HS = headspace. Only a portion of this table appears here. The complete table is available in [ASCII format](#).

Table T3. Site 1147 composite depths.

Core	Depth (mbsf)	Cumulative offset (m)	Depth (mcd)
184-1147A-			
1H	0.0	0.15	0.15
2H	5.4	1.45	6.85
3H	14.9	1.75	16.65
4H	24.4	2.95	27.35
5H	33.9	2.90	36.80
6H	43.4	4.25	47.65
7H	52.9	5.35	58.25
8H	62.4	7.15	69.55
9H	71.9	7.65	79.55
184-1147B-			
1H	0.0	0.00	0.00
2H	9.5	0.50	10.00
3H	19.0	1.30	20.30
4H	28.5	1.70	30.20
5H	38.0	1.90	39.90
6H	47.5	3.35	50.85
7H	57.0	4.90	61.90
8H	66.5	6.20	72.70
9H	76.0	6.20	82.20
184-1147C-			
1H	0.0	0.05	0.05
2H	2.6	0.60	3.20
3H	12.1	0.45	12.55
4H	21.6	2.05	23.65
5H	31.1	2.18	33.28
6H	40.6	3.00	43.60
7H	50.1	4.05	54.15
8H	59.6	5.55	65.15
9H	69.1	6.10	75.20

Note: This table is also available in [ASCII format](#).

Table T4. Site 1147 splice tie points.

Hole, core, section, interval (cm)	Depth			Hole, core, section, interval (cm)	Depth	
	(mbsf)	(mcd)			(mbsf)	(mcd)
184-				184-		
1147B-1H-1, 0	0.00	0.00				
1147B-1H-6, 12	7.62	7.62	Tie to	1147C-2H-3, 142	7.02	7.62
1147C-2H-6, 112	11.22	11.82	Tie to	1147B-2H-2, 32	11.32	11.82
1147B-2H-6, 92	17.92	18.42	Tie to	1147A-3H-2, 27	16.67	18.42
1147A-3H-6, 107	23.47	25.22	Tie to	1147C-4H-2, 7	23.17	25.22
1147C-4H-5, 82	28.42	30.47	Tie to	1147B-4H-1, 27	28.77	30.47
1147B-4H-5, 62	35.12	36.82	Tie to	1147C-5H-3, 52	34.64	36.82
1147C-5H-6, 92	39.54	41.72	Tie to	1147B-5H-2, 32	39.82	41.72
1147B-5H-5, 96	44.96	46.86	Tie to	1147C-6H-3, 25	43.86	46.86
1147C-6H-6, 142	49.52	52.52	Tie to	1147B-6H-2, 17	49.17	52.52
1147B-6H-4, 32	52.32	55.67	Tie to	1147C-7H-1, 152	51.62	55.67
1147C-7H-7, 47	59.57	63.62	Tie to	1147B-7H-2, 22	58.72	63.62
1147B-7H-4, 42	61.92	66.82	Tie to	1147C-8H-2, 17	61.27	66.82
1147C-8H-6, 72	67.82	73.37	Tie to	1147B-8H-2, 52	67.17	73.37
1147B-8H-5, 142	72.57	78.77	Tie to	1147C-9H-3, 57	72.67	78.77
1147C-9H-6, 137	77.97	84.07	Tie to	1147B-9H-2, 37	77.87	84.07
1147B-9H-6, 128	84.53	90.73				

Note: This table is also available in [ASCII format](#).

Table T5. Light-colored, carbonate-rich layers observed in cores recovered at Site 1147.

Core, section interval (cm)	Top		Bottom		Thickness (cm)
	Depth (mbsf)	Depth (mcd)	Depth (mbsf)	Depth (mcd)	
184-1147A-					
1H-1, 0-70	0.00	0.15	0.70	0.85	70
2H-6, 100-150	13.90	15.35	14.40	15.85	50
3H-1, 0-29	14.90	16.65	15.19	16.94	29
4H-2, 88-138	26.78	29.73	27.28	30.23	50
4H-6, 48-110	32.38	35.33	33.00	35.95	62
5H-2, 66, to 5H-4, 86	36.06	38.96	39.26	42.16	320
6H-2, 80, to 6H-3, 90	45.70	49.95	47.30	51.55	160
184-1147B-					
1H-1, 0-80	0.00	0.00	0.80	0.80	80
2H-4, 24, to 2H-5, 30	14.24	14.74	15.80	16.30	156
3H-5, 93-145	25.93	27.23	26.45	27.75	52
4H-6, 84, to 4H-7, 12	36.84	38.54	37.62	39.32	78
5H-5, 135, to 5H-CC, 21	45.35	47.25	47.32	49.22	117
6H-1, 0-60	47.50	50.85	48.10	51.45	60
7H-5, 112-150	64.12	69.02	64.50	69.40	38
8H-4, 3-105	69.68	75.88	70.70	76.90	102
8H-5, 43-115	71.58	77.78	72.30	78.50	72
9H-2, 5-58	77.55	83.75	78.08	84.28	53
9H-4, 2-45	80.27	86.47	80.70	86.90	43
184-1147C-					
1H-1, 0-80	0.00	0.05	0.80	0.85	80
2H-4, 10-115	7.20	7.80	8.25	8.85	105
3H-2, 105, to 3H-3, 70	14.65	15.10	15.80	16.25	115
4H-3, 55-94	25.15	27.20	25.54	27.59	39
4H-5, 19-60	27.79	29.84	28.20	30.25	41
5H-4, 11-49	35.73	37.91	36.11	38.29	38
5H-4, 86-140	36.48	38.66	37.02	39.20	54
5H-5, 50-109	37.62	39.80	38.21	40.39	59
5H-6, 50-91	39.12	41.30	39.53	41.71	41
6H-5, 47, to 6H-6, 40	47.07	50.07	48.50	51.50	143
8H-3, 130, to 8H-4, 70	63.90	69.45	64.80	70.35	90

Table T6. Volcanic ash layers recovered at Site 1147.

Core, section interval (cm)	Top		Bottom		Thickness (cm)	Remarks/comments
	Depth (mbsf)	Depth (mcd)	Depth (mbsf)	Depth (mcd)		
184-1147A-						
1H-4, 30-64	4.80	4.95	5.14	5.29	34	Round burrows filled with light gray volcanic ash
2H-5, 89	12.29	13.74	12.29	13.74	<1	Light gray volcanic ash filling round burrows
4H-2, 126	27.16	30.11	27.16	30.11	<1	White ash layer
6H-2, 40-46	45.30	49.55	45.36	49.61	6	Brownish gray volcanic ash filling burrows
6H-2, 77-78	45.67	49.92	45.68	49.93	1	White ash layer
6H-2, 80-82	45.70	49.95	45.72	49.97	2	Brownish ash layer
184-1147B-						
1H-3, 144, to 1H-4, 8	4.44	4.44	4.58	4.58	24	Round burrows filled with light gray volcanic ash
1H-6, 5	7.55	7.55	7.55	7.55	<1	Light gray volcanic ash filling round burrows
2H-5, 88	16.38	16.88	16.38	16.88	<1	Light gray volcanic ash filling round burrows
4H-1, 9	28.59	30.99	28.59	30.99	<1	Light gray volcanic ash filling round burrows
4H-4, 59	33.59	35.29	33.59	35.29	1	Dark brown ash layer
6H-2, 3	49.03	52.38	49.03	52.38	<1	Pumice fragment
184-1147C-						
2H-2, 91-131	5.01	5.61	5.41	6.01	40	Zone of ash-filled burrows
4H-5, 44-72	28.04	30.09	28.32	30.37	28	Zone of ash-filled burrows
5H-3, 130-132	35.42	37.60	35.44	37.62	2	Dispersed fine-grained dark gray ash
6H-5, 3-13	46.63	49.63	46.73	49.73	10	Round burrows filled with light gray volcanic ash
6H-5, 38-45	46.98	49.98	47.05	50.05	7	Round burrows filled with light gray volcanic ash

Table T7. Summary of biohorizons at Site 1147.

Code	Events	Depth range of stratigraphic datums						Average depth (mcd)	Age (Ma)	Average sedimentation rate (m/m.y.)
		Top			Bottom					
		Core, section, interval (cm)	Depth (mbsf)	Depth (mcd)	Core, section, interval (cm)	Depth (mbsf)	Depth (mcd)			
		184-1147A-			184-1147A-					
PF	LO pink <i>G. ruber</i>	1H-CC, 0-10	5.23	5.43	2H-CC, 7-15	14.48	15.98	10.71	0.12	
CN	FO <i>E. huxleyi</i>	3H-CC, 16-22	24.67	26.42	4H-CC, 9-14	33.98	36.81	31.62	0.26	74
PF	FO pink <i>G. ruber</i>	3H-CC, 16-22	24.67	26.42	4H-CC, 9-14	33.98	36.81	31.62	0.40	
CN	LO <i>P. lacunosa</i>	3H-CC, 16-22	24.67	26.42	4H-CC, 9-14	33.98	36.81	31.62	0.46	
BF	LO <i>Stilostomella</i>	6H-CC, 0-6	52.29	56.51	7H-CC, 18-24	62.68	68.06	62.29	0.75	
CN	LO <i>Reticulofenestra asanoi</i>	6H-CC, 0-6	52.29	56.51	7H-CC, 18-24	62.68	68.06	62.29	0.83	
CN	LO small <i>Gephyrocapsa acme</i> *	8H-2, 140	66.80	73.95	8H-3, 140	68.30	75.45	74.70	1.01	
CN	FO small <i>Gephyrocapsa acme</i>	8H-CC, 16-22	71.66	78.84	9H-CC, 16-22	81.77	89.39	84.12	1.22	45

Notes: Sources of reference age for all biostratigraphic events are listed in Tables T2, p. 42, and T3, p. 43, in the "Explanatory Notes" chapter. CN = calcareous nannofossils, PF = planktonic foraminifers, BF = benthic foraminifers, FO = first occurrence, LO = last occurrence. * = events used in calculating average sedimentation rate. Depth for the top and bottom of biostratigraphic events = the mean of the sample interval. Depth in bold indicates where datum is recorded; depth range between the top and bottom is the interval where the real bioevent may occur. Bar in average sedimentation rate column indicates the range of samples to which the average sedimentation rate applies.

Table T9. Planktonic foraminifer checklist for Site 1147.

Epoch	Zone	Core, section, interval (cm)	Depth (mcd)	Abundance	Preservation	<i>Globorotalia crassaformis</i>	<i>Globorotalia inflata</i>	<i>Globorotalia menardii</i>	<i>Globorotalia truncatulinoides</i>	<i>Globigerinoides ruber</i>	<i>Globigerinoides ruber</i> (pink)	<i>Neogloboquadrina acostaensis</i>	<i>Neogloboquadrina dutertrei</i>	<i>Pulleniatina obliquiloculata</i>	
Pleistocene	N22	184-1147A-1H-CC, 0-10	5.43	A	VG	F	P		A					R	
		2H-CC, 7-15	15.98	A	VG	R	F		F		R			A	
		3H-CC, 16-22	26.42	A	G	A			A		R		F	A	
		4H-CC, 9-14	36.95	A	VG	R	A			A	P		F	A	
		5H-CC, 16-21	46.58	A	VG		R		P	A					F
		6H-CC, 0-6	56.57	A	M	R			R	A					F
		7H-CC, 18-24	68.06	A	VG				R					R	F
		8H-CC, 16-22	78.84	A	M				R			R			
		9H-CC, 19-25	89.39	A	P	R			R						A

Notes: A = abundant, F = few/frequent, R = rare, VG = very good, G = good, M = moderate, P = poor. See "Biostratigraphy," p. 9, in the "Explanatory Notes" chapter.

Table T10. Age-depth relationship derived from the magnetic polarity time scale, Site 1147.

Polarity event	Age (Ma)	Depth (mcd)			Average depth (mcd)
		Hole 1147A	Hole 1147B	Hole 1147C	
Brunhes/Matuyama	0.78	59.3	57.4	57.0	57.9
upper Jaramillo	0.99	72.0	70.8	72.3	71.7
lower Jaramillo	1.07	76.1	76.1	76.1	76.1

Table T11. Sedimentation and accumulation rates for selected intervals, based on age-depth model and rates presented in Figure **F11**, p. 21.

	Bottom of interval		LSR total (m/m.y.)	LSR carbonate (m/m.y.)	MAR total (g/cm ² /k.y.)	MAR carbonate (g/cm ² /k.y.)
	Age (Ma)	Depth (mcd)				
NN21/NN20	0.26	24.8	96	11.6	5.7	0.68
Brunhes/Matuyama	0.78	57.9	65	9.8	4.9	0.72
Bottom of hole	1.34	90.8	56	6.5	5.7	0.66

Note: LSR = linear sedimentation rate for total sediment and inorganic carbonate, MAR = mass accumulation rate for total sediment and inorganic carbonate.

Table T12. Inorganic carbon, carbonate, total carbon, total organic carbon, total nitrogen, and total sulfur contents at Site 1147.

Core, section, interval (cm)	Depth		IC (wt%)	CaCO ₃ (wt%)	TC (wt%)	TOC (wt%)	TN (wt%)	TS (wt%)	C/N
	(mbsf)	(mcd)							
184-1147A-									
1H-2, 107-108	2.57	2.72	1.15	9.5	2.36	1.21	0.19	0.30	6.3
2H-2, 107-108	7.97	9.42	2.30	19.1	3.24	0.95	0.13	0.45	7.6
2H-4, 107-108	10.97	12.42	0.62	5.1	1.19	0.58	0.13	0.20	4.4
2H-6, 107-108	13.97	15.42	2.22	18.5					
3H-2, 107-108	17.47	19.22	1.08	9.0					
3H-4, 107-108	20.47	22.22	1.45	12.1	2.01	0.56	0.09	0.30	6.5
3H-6, 107-108	23.47	25.22	0.53	4.4					
4H-2, 107-108	26.97	29.92	2.27	18.9					
4H-4, 107-108	29.97	32.92	2.09	17.4	2.85	0.76	0.15	0.60	5.1
4H-6, 107-108	32.97	35.92	3.66	30.5					
5H-2, 107-108	36.47	39.37	1.76	14.7					
5H-4, 107-108	39.47	42.37	2.13	17.7	2.50	0.37	0.09	0.30	4.4
5H-6, 107-108	42.47	45.37	1.74	14.5					
6H-2, 107-108	45.97	50.22	1.30	10.8					
6H-4, 107-108	48.97	53.22	0.80	6.7	1.18	0.38	0.12	0.08	3.3
6H-6, 107-108	51.97	56.22	0.65	5.4					
7H-2, 107-108	55.47	60.82	1.36	11.3					
7H-4, 107-108	58.47	63.82	1.48	12.4	1.62	0.14	0.11	0.40	1.3
7H-6, 107-108	61.47	66.82	2.01	16.8					
8H-2, 107-108	64.97	72.12	0.76	6.3					
8H-4, 107-108	67.97	75.12	0.94	7.8	1.22	0.29	0.12	0.00	2.5
9H-2, 107-108	74.47	82.12	1.69	14.1					
9H-4, 107-108	77.47	85.12	1.60	13.4	1.95	0.34	0.07	0.10	4.9
9H-6, 107-108	80.47	88.12	1.38	11.5					

Note: IC = inorganic carbon, CaCO₃ = carbonate, TC = total carbon, TOC = total organic carbon, TN = total nitrogen, TS = total sulfur, C/N = carbon/nitrogen ratio.

Table T13. Composition of interstitial waters in Hole 1147A.

Core, section, interval (cm)	Depth		pH	Alkalinity (mM)	Salinity	Cl ⁻ (mM)	Na ⁺ (mM)	K ⁺ (mM)	Mg ²⁺ (mM)	Ca ²⁺ (mM)	SO ₄ ²⁻ (mM)	HPO ₄ ²⁻ (μM)	NH ₄ ⁺ (μM)	H ₄ SiO ₄ (μM)	Li ⁺ (μM)	Sr ²⁺ (μM)
	(mbsf)	(mcd)														
184-1147A-																
1H-2, 145-150	2.98	3.13	7.51	5.12	35	545	463	11.7	52.9	11.1	26.6	26.3	99	603	27	86
2H-3, 145-150	9.88	11.33	7.51	9.86	34	556	474	12.2	51.6	8.8	21.2	47.7	406	666	24	89
3H-3, 145-150	19.38	21.13	7.26	11.83	34	559	478	11.4	51.4	8.0	19.2	44.4	436	722	26	90
4H-3, 145-150	28.88	31.83	7.26	11.54	34	557	474	11.2	50.8	8.1	17.7	26.3	485	769	29	95
5H-3, 145-150	38.38	41.28	7.39	11.06	34	561	480	11.2	49.0	7.7	16.9	16.1	491	635	32	104
7H-3, 145-150	57.38	62.73	7.37	9.51	34	559	477	10.2	47.4	7.3	15.0	7.6	525	344	33	116
9H-3, 145-150	76.38	84.03	7.34	8.13	34	558	478	8.9	46.1	7.1	14.0	0.7	496	201	28	153